Evaluating the Performance of Bioswales Using a Hydrological Groundwater Model

Insights from a Rotterdam Case Study

Master's Thesis

E.I. Oosterveld

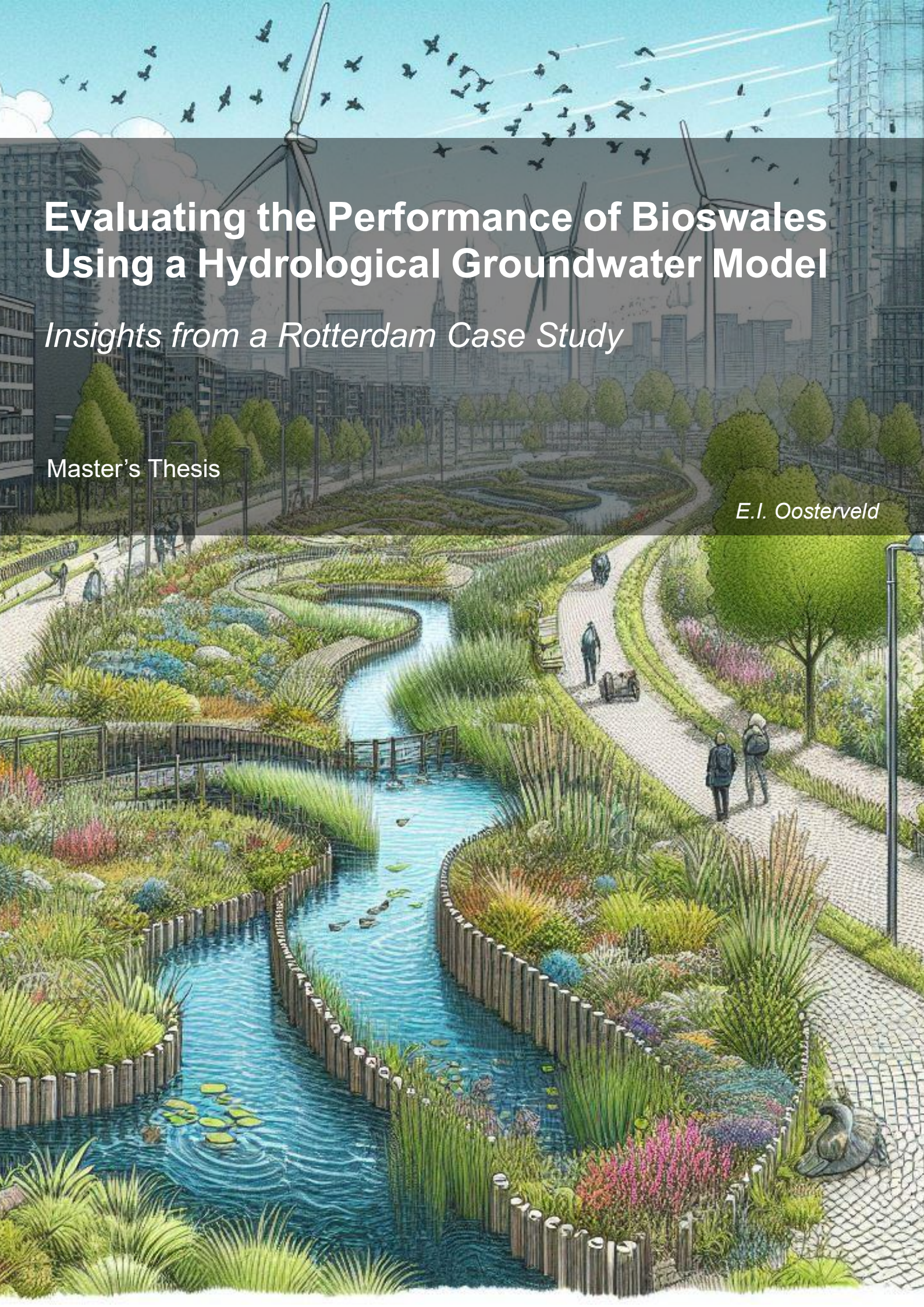

Evaluating the Performance of Bioswales Using a Hydrological Groundwater Model

Insights from a Rotterdam Case Study

Master's Thesis

By

E.I. Oosterveld

in partial fulfilment of the requirements for the degree of

Master of Science
in Environmental Engineering

at the Delft University of Technology,
to be defended publicly on November 28th, 2024

Graduation Committee

First Supervisor, TU Delft	Prof. Dr. Z. Kapelan
Second Supervisor, TU Delft	Prof. Dr. T. A. Bogaard
External Supervisor, Municipality of Rotterdam	Ir. G. van der Hout
External Supervisor, Municipality of Rotterdam	Dr. Ir. N. Stanić

Cover image by:
Microsoft Bing Image Creator

TU Delft

Gemeente Rotterdam

Preface

This thesis concludes my Master of Science in Environmental Engineering with a speciality in Water Resources Engineering at Delft University of Technology, marking the end of my time as a student in Delft. My research explored the hydrological modelling of bioswales, combining my interest in natural and urban water systems with climate change impacts, modelling, and data analysis. I look forward to continuing to work in this field!

This thesis was made possible with the involvement of individuals from both the Municipality of Rotterdam and TU Delft. First, I would like to thank Nikola Stanić and Ella van der Hout from IBR for providing me with the resources to conduct this research and for our constructive weekly meetings. Your expertise and questions helped me develop a critical perspective on my work and guided me through the various stages of the thesis execution. I also appreciate the support from the team of colleagues at the Municipality of Rotterdam, who were always available to discuss specific questions and offered insightful ideas. Thanks also go to my TU Delft graduation committee members, Zoran Kapelan and Thom Bogaard, for your guidance, motivational meetings, and helpful feedback.

I would like to thank my family and friends who supported me throughout my time studying at TU Delft, especially during this final stage of completing my thesis. I am grateful to my parents for keeping me motivated and for their willingness to proofread my work and discuss my research approach, even without a background in this field. To my friends, thank you for providing much-needed distractions and a listening ear when I needed it most.

Emma Oosterveld
Delft, November 2024

Abstract

The expected effects of climate change on increased and more frequent rainfall events ask for more innovative solutions to manage urban stormwater. Sustainable Urban Drainage Systems (SuDS) offer an eco-friendly method to disconnect stormwater from the sewer system. The Municipality of Rotterdam, the Netherlands, has integrated multiple SuDS into its drainage network, including bioswales. Bioswales are vegetated areas that slow down, collect, and filter (storm) runoff. However, uncertainty exists regarding their performance under different conditions. This thesis aims to answer the following research question: How do bioswales perform under various conditions, as evaluated by a hydrological groundwater model?

The bioswale groundwater model used in this thesis, developed by Deltares, utilizes the Unsaturated Zone Flow (UZF) package of MODFLOW to simulate the hydrological response of bioswales. The model was calibrated and validated using existing monitoring data, and a *one-at-a-time* sensitivity analysis was performed to identify the most influential factors affecting bioswale performance. The case-study bioswale was tested under design storms reflecting current and 2050 summer and winter conditions, as well as prolonged wet winter rainfall. Two design scenarios were proposed to improve bioswale performance.

The case-study calibration results showed that the model could realistically simulate water levels and discharges. However, the existence of preferential flow in the unsaturated zone, not accounted for by the UZF package, led to a time-lag in modelled drain discharge. The sensitivity analysis indicated that infiltration parameters strongly influence emptying time, peak discharge, and time-lag in the model. The performance assessment showed that the case-study bioswale met the emptying time criterion, but the peak discharge limit was exceeded during summer events. Simulating prolonged wet winter rainfall showed that consecutive rainfall events could be more critical regarding winter bioswale performance, compared to a single winter design storm. The bioswale design improvements demonstrated that relocating the drain from the centre to the side of the bioswale, thereby increasing the distance water needs to travel, significantly reduced peak discharge, though at the cost of longer emptying times. Widening the bioswale increased storage volume; therefore, the connected paved surface area could be increased, but the effect of adding additional drains on bioswale performance was limited.

To increase the understanding of bioswale performance, further empirical research on vegetation, macropores, and preferential flow is recommended, along with improvements to the modelling of these processes. In terms of model application, the bioswale groundwater model, with some adjustments, can be applied to other SuDS types that might be less sensitive to the natural influences of vegetation change and macropores. Combining the modelling of individual bioswales and SuDS, as done in this study, with urban-scale modelling could significantly improve Rotterdam's climate resilience.

Table of contents

1. Introduction

1.1 Motivation

Over the past decades, human behaviour has enhanced the greenhouse effect and thereby global warming. One of the effects of climate change is an increase in rainfall (IPCC, 2023). Moreover, heavy rainfall events are expected to increase significantly in both frequency and magnitude throughout most of Europe with an expected increased global temperature of 1.5°C (IPCC, 2023). According to the *Royal Netherlands Meteorological Institute* (KNMI, in Dutch: *Koninklijk Nederlands Meteorologisch Instituut*), the frequency of extreme rainfall in the Netherlands has already seen an increase as a result of human-induced climate effects (KNMI, 2023). Furthermore, in every climate scenario of the KNMI, winter rainfall is expected to increase, as well as the magnitude and frequency of extreme rainfall events in summer months. When considering that the Netherlands is characterized by the concentration of population in urban areas and accordingly the cities' high degree of petrification, the cities in the Netherlands become increasingly vulnerable to urban (pluvial) flooding caused by heavy rainfall (Bouwens et al., 2018). This, in turn, threatens the cities' infrastructure, the economy and the lives of the citizens (Hurford et al., 2012; Spekkers et al., 2015).

Rotterdam, the second largest city in the Netherlands and situated near the west coast, is particularly vulnerable to flooding due to its high groundwater levels. Bouwens et al. (2018) found in their study a strong correlation between flooding and maximum rainfall depth in Rotterdam. Given these challenges, urban areas like Rotterdam need innovative solutions to manage stormwater more effectively. Sustainable Urban Drainage Systems (SuDS) offer an alternative to traditional urban stormwater system design and disconnect stormwater runoff from the sewer system in an eco-friendly and natural manner. The main goals of SuDS are to reduce the stormwater peak and to delay runoff to the sewer system and surface water. This is illustrated in Figure 1.1 below.

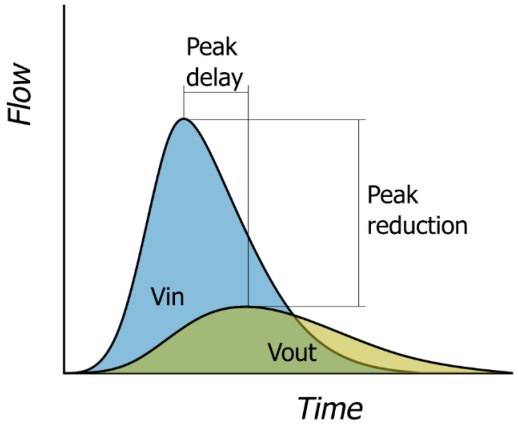

Figure 1.1: Peak reduction and peak delay illustration (Metz, 2022)

1.2 Introduction to bioswales

Many types of SuDS exist, of which the focus of this research will be on bioswales as they are a popular solution implemented by the municipality of Rotterdam. Bioswales (see Figure 1.2) are engineered, vegetated shallow depressions that slow down, collect, and filter stormwater runoff from surrounded vegetated areas and impervious surfaces, such as roads and rooftops. They are designed with soil layers that promote infiltration while also storing water in the swale to delay the stormwater peak. Additionally, bioswales can be equipped with drainage systems to transport water

to the stormwater system or surface water. To prevent bioswales from spilling over, an outlet that is directly connected to the drainage or stormwater system can be incorporated into the design (see Figure 1.2). Section 2.1 provides a more detailed description of the design and performance requirements of bioswales in Rotterdam.

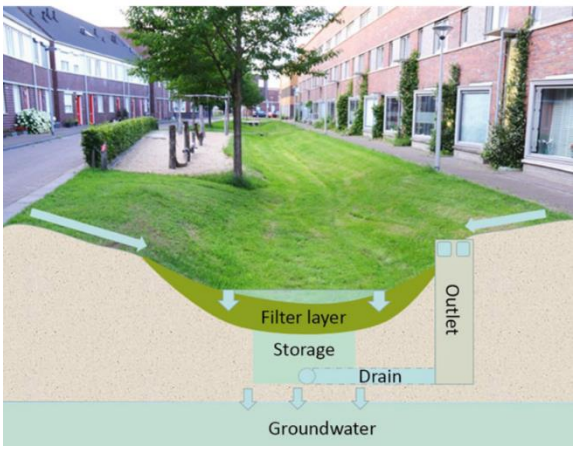

Figure 1.2: Cross-section of a bioswale (Koning & Boogaard, 2023)

1.3 Problem statement

Bioswales are increasingly being implemented in urban areas like Rotterdam as part of flood mitigation strategies. However, much uncertainty and unclarity still exist concerning their performance. Specifically in delta areas characterized by high groundwater tables and poorly permeable soils, like Rotterdam, their efficacy is often questioned (Boogaard, 2015). Therefore, it is necessary to better understand the performance of bioswales to effectively address the anticipated increase in rainfall due to climate change.

The use of hydrological models can aid in the assessment of the performance of bioswales. Models allow testing different kinds of variables, some of which are challenging to measure through monitoring and are characterized by high uncertainty (Kumar et al., 2021). With the use of hydrological models, the response of bioswales can be tested under different extreme weather conditions or to predict their performance under future projected rainfall extremes. Urban hydrology-hydraulic models, such as the Storm Water Management Model (SWMM) and Infoworks ICM, are widely used for simulating SuDS and bioswales at catchment scales. These models, though effective for large-scale urban flooding simulations, fall short in detailed modelling of the complex hydrological processes within individual bioswales. For example, they do not effectively simulate multiple soil layers or groundwater responses (Kaykhosravi et al, 2018).

To overcome these limitations and to accurately simulate bioswale performance, a more detailed hydrological model is required—one that integrates both the unsaturated and saturated zones. The finite difference groundwater model MODFLOW is widely used for simulating groundwater flow and includes an Unsaturated-Zone Flow (UZF) package to account for vertical water movement in the unsaturated zone. However, despite its potential, the application of MODFLOW with the UZF package to model SuDS, particularly bioswales, is limited. Most studies, such as those by Zell et al. (2015), Hunt et al. (2008), and Leterme et al. (2015), have focused on applying the UZF package to large-scale groundwater systems spanning square kilometres and simulating over extended periods, rather than on the small-scale, detailed analysis required for bioswales. This thesis uses a hydrological groundwater model that makes use of the UZF package of MODFLOW. By modelling the interaction between the unsaturated and saturated zones, this research aims to provide a more accurate understanding of bioswale functionality. These insights can enhance the effectiveness of bioswale designs and contribute to the city's climate adaptation strategies.

1.4 Research objective and questions

This research aims to determine the performance of bioswales using a hydrological groundwater model that incorporates simulation of unsaturated zone flow processes. The study is carried out to further understand the performance of bioswales, their limitations and potentials; ultimately this knowledge can help to better define the city's climate adaptation strategies. Consequently, the following main research question transpired:

How do bioswales perform under various conditions, as evaluated by a hydrological groundwater model?

To answer the main research question, the following sub-questions are defined:

1. How accurately does the groundwater model simulate the hydrological response of a bioswale?
2. What are the critical factors influencing the performance of bioswales?
3. How do bioswales perform under different representative weather and climate conditions?
4. Can the existing bioswale design be improved to better meet performance requirements?

1.5 Research scope and approach

This research focuses on evaluating the performance of bioswales in the Municipality of Rotterdam using a hydrological groundwater model developed by Deltares. The model uses the UZF package of MODFLOW and models the unsaturated and the saturated zones and will be referred to as the bioswale groundwater model throughout this thesis. This research will focus on the urban flood mitigation function of bioswales, other functions such as water quality and biodiversity improvement will not be covered in this study.

The study is focusing on the representative bioswale in Rotterdam's case study area with available monitoring data. The first research question will be answered by calibrating and validating the bioswale groundwater model with measurement data of full-scale tests. Further, a sensitivity analysis will be conducted on model parameters to answer the second sub-question. Further, design storms for winter and summer conditions in current and future climates are used to test the performance of the case-study bioswale. Finally, the performance of different design scenarios in terms of drain location, bioswale size and soil composition will be evaluated.

1.6 Thesis structure

The outline of the thesis is structured as follows. **Chapter 1** introduces the current climate adaptation challenges in urban environments and defines the objective of this research thesis. **Chapter 2** provides background information on the design and performance of bioswales and groundwater flow processes. **Chapter 3** presents the methodology used to answer the research questions and applied to the case-study bioswale. **Chapter 4** presents data and model conceptualisation of the selected case-study bioswale area in Rotterdam. The research results and discussion can be found in **Chapter 5**. Finally, **Chapter 6** presents the conclusions of this study and recommendations for future work.

2. Background

This chapter describes background information based on literature about the design and performance of bioswales and the theory behind groundwater flow in saturated and unsaturated zones.

2.1 Bioswales

2.1.1 Design of bioswales in Rotterdam

The subsoil in Rotterdam consists of poorly permeable clay and peat layers, which allow for localized water retention using bioswales. Over the past years, the municipality has constructed numerous SuDS, including tens of bioswales across the city. The bioswales in Rotterdam are designed according to the bioswale guidelines of the municipality, the 'Rotterdamse wadi bouwsteen' (Mobron, 2024). The design and performance criteria used in this study are based on this document.

The bioswales in Rotterdam are designed to serve two main functions:

- **Storage**
  Rainfall and runoff are temporarily stored in the aboveground section of the bioswale, before it leads to groundwater recharge, resulting in delay and reduction of the incoming (storm) peak.

- **Drainage**
  Excess infiltrated water is directed to the sewer system or surface waters, reducing local flooding.

Figure 2.1 shows a typical bioswale design used within the Municipality of Rotterdam, where the storage and drainage functions are clearly visible.

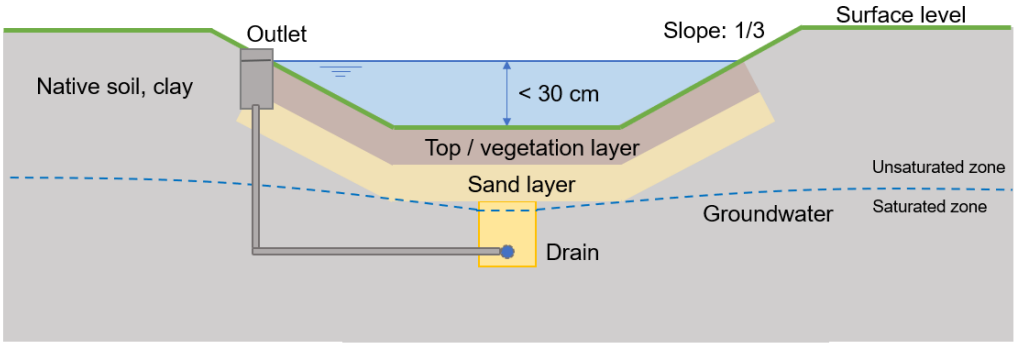

Figure 2.1: Cross section of typical bioswale design in Rotterdam

The following principles are considered in the bioswale design shown in Figure 2.1:

- **Dimension**
  The side of bioswales is designed with a sloping embankment, to maintain a shallow layer of water (Davis, 2018; Woods Ballard et al., 2015). The slope should not be too steep to

ensure that people can safely climb out of the bioswale. In the Rotterdam bioswale design, the slope must not exceed a 1:3 ratio (see Figure 2.1). Furthermore, the shape of the bioswale influences the maximum volume, connected paved surface area and infiltration (Koning & Boogaard, 2023).

- **Soil layers**
  The native soil in areas where bioswales are constructed often requires improvement, as the clay soil in Rotterdam is not permeable enough. The top layer has an increased permeability to facilitate infiltration. Vegetation is rooted in this top layer (Davis, 2018). The composition of this top layer is crucial. During design, it is important to avoid overly high permeability, which would reduce the bioswale's storage capacity. However, permeability should not be too low, as this could lead to overflow or prolonged water ponding in the bioswale. The permeability of the top layer is influenced by natural factors such as seasonal changes in vegetation and soil biology (see section 2.1.3). The Municipality of Rotterdam recommends a hydraulic conductivity based on soil texture of 0.5 m/d for the improved top layer, which typically decreases to 0.3 m/d over the bioswale's lifetime due to compaction and vegetation growth (Mobron, 2024).
  The layer beneath the top layer is primarily composed of sand, which promotes drainage. Due to the low permeability of the surrounding native soil, lateral water movement to surrounding areas is expected to be limited (Mobron, 2019; Mobron, 2024).

- **Vegetation**
  The type of vegetation in the bioswale influences the infiltration. Higher and denser grass types can help in slowing down infiltration (Koning & Boogaard, 2023), while root growth can help improve permeability of the soil, through the creation of macropores (Lewis et al., 2008).

- **Engineered elements**
  Due to Rotterdam's high groundwater table, bioswales are designed with drains (Mobron, 2024). The drain functions as follows. When the infiltrated water reaches the groundwater table, the groundwater level will rise. When the groundwater level rises above the set drainage level, the excess groundwater is drained away. Depending on the bioswale's size and soil types, multiple drains may be used to ensure proper drainage.
  An overflow can be incorporated as a safety measure to prevent the water depth in the bioswale from exceeding its maximum value.

2.1.2 Performance requirements

To assess the performance of bioswales under different conditions, performance indicators must be defined. Davis (2008) defined performance indicators for testing raingardens based on volume reduction, peak reduction, and peak delay. The Municipality of Rotterdam has established its own criteria for the design of bioswales, which indirectly represent the three indicators defined by Davis (2008). These criteria (Mobron, 2024), which assess both the storage and drainage functions of bioswales, are as follows (see also Figure 2.2 and 2.3).

- **Emptying time < 36 hours**
  The emptying time of a full bioswale must be less than 36 hours to enhance infiltration. Prolonged emptying times can damage the vegetation in the bioswale. The emptying time is defined as the period from the end of the rainfall event until the bioswale is fully emptied (see Figure 2.2).

- **Maximum water depth (W_{max}) < 30 cm**
  In Rotterdam, the water depth in bioswales should not exceed 30 cm (as illustrated in the bioswale cross-section in Figure 2.1 and graphically in Figure 2.2) as this could pose a

safety risk for children or people who might fall into the bioswale. To manage this, an overflow is typically installed at the maximum allowed water depth. The size and runoff area of bioswales are designed so that the swale is filled (to 30 cm) during a design storm with a return period of two years.

- **Peak discharge ($Q_{peak, out}$) < 2 L/s/ha**
  Waterboards have an important role regarding flood safety in the Netherlands. The "*Waterschap Hollandse Delta"* imposes discharge requirements, allowing a maximum peak discharge of 2 L/s/ha for surface waters in Rotterdam (Waterschap Hollandse Delta, 2020). This value serves as the upper limit for the peak drain discharge bioswales. This value is calculated as a ratio of maximum drain outflow ($Q_{peak,out}$ in Figure 2.3) and total runoff area.

- **Maximum return period flooding swale = 2 years**
  According to the bioswale guidelines of the Municipality of Rotterdam, a rainfall event with a return period of 2 years should not cause any flooding or overflow. This means that during an event with a return period of 2 years, a bioswale must not overspill.

- **Maximum ponding duration of bioswale = 7 days**
  To prevent the formation of mosquitoes, standing water in the swale must not exceed a duration of 7 days during summer, as mosquito eggs can develop into adults within this time frame.

- **Volume reduction**
  As described by Davis (2008), bioswale performance can also be assessed based on volume reduction, comparing the volume of water entering the bioswale to the volume discharged through the drain (see Figure 2.3). A higher volume reduction is considered more desirable. However, the Municipality of Rotterdam does not have specific criteria for this value. Nonetheless, volume reduction will be calculated as follows:

$$f_V = \frac{V_{out}}{V_{in}}$$

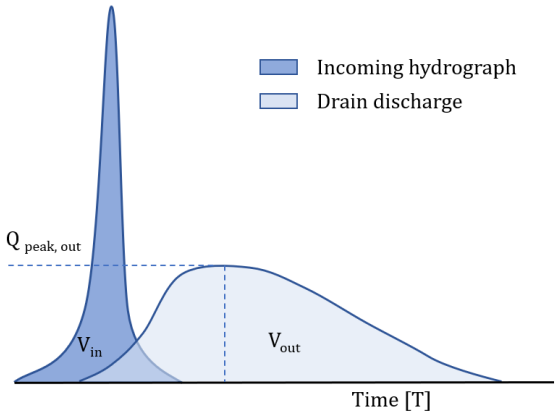

Figure 2.3: Visual representation of performance indicators regarding drain discharge (not on scale)

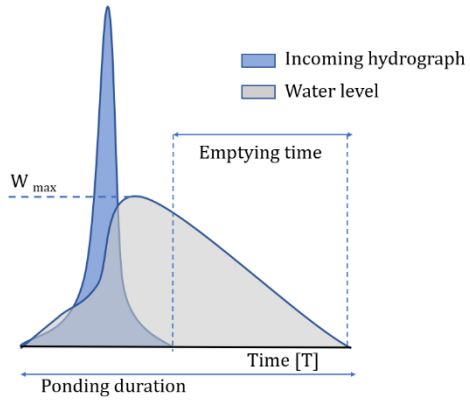

Figure 2.2: Visual representation of performance indicators regarding water level in the bioswale (not on scale)

2.1.3 Temporal and spatial variation of performance of bioswales

The performance of bioswales (and other SuDS) is generally assessed through full-scale tests or during rainfall events. Most measurement campaigns focus on testing the infiltration rates of bioswales (and SuDS in general). As noted by Ebrahimian et al. (2020), infiltration is the primary factor influencing SuDS performance. However, infiltration measurements have shown a high degree of spatial and temporal variability in the hydraulic performance of bioswales, as seen in the studies of Koning & Boogaard (2023), Boogaard (2022), and Kondratenko et al. (2024). Koning & Boogaard (2023) compiled data from various full-scale bioswale measurement campaigns in the Netherlands. Their findings, shown in Figure 2.4, reveal significant variability in the infiltration rates of the tested bioswales.

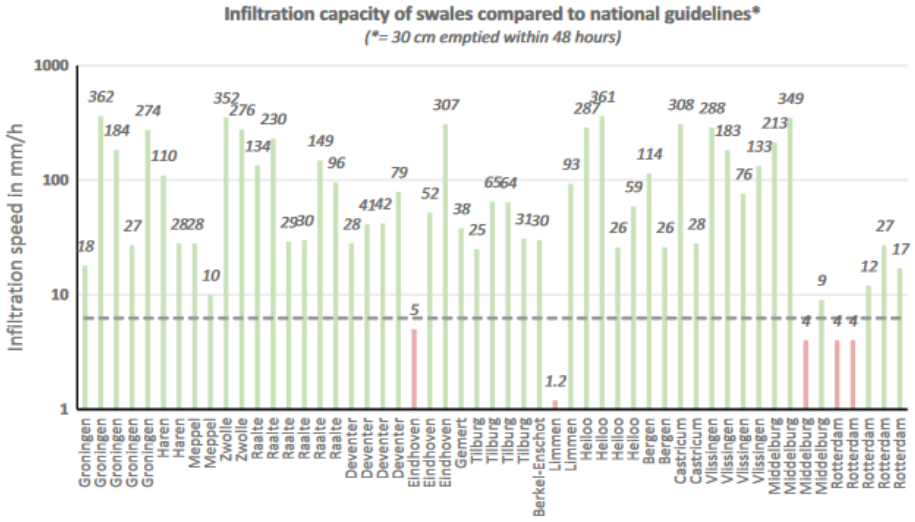

Figure 2.4: Variation of measured infiltration rates of bioswales in the Netherlands (Koning & Boogaard, 2023))

Boogaard (2022) measured the infiltration rates of three bioswales in Dalfsen, the Netherlands, with a focus on their performance under drought conditions. Initial infiltration capacities ranged from 66,7 mm/h to 496 mm/h, with higher rates observed in dry initial conditions.

Kondratenko et al. (2024) examined the spatial and temporal variation in bioswale infiltration rates in Riga, Latvia. They found that infiltration rates varied from 4.5 to 320 mm/h, even for bioswales with similar designs. Furthermore, after soil saturation, infiltration capacity decreased by 30% to 58%. The tests also revealed a 25% to 50% reduction in infiltration rates in October compared to July.

Infiltration rates are primarily influenced by soil hydraulic conductivity. Ebrahimian et al. (2020) conducted an extensive review of the spatial and temporal variability of hydraulic conductivity in SuDS. Hydraulic conductivity can fluctuate over time due to several factors. The flowchart in Figure 2.5 below, obtained from Ebrahimian et al. (2020), highlights various contributors to changes in hydraulic conductivity. A decrease in conductivity can result from factors such as clogging by fine plant roots and soil compaction during construction and maintenance. On the other hand, an increase can occur due to reduced water viscosity from higher temperatures and increased macroporosity from plant root growth and biological activity.

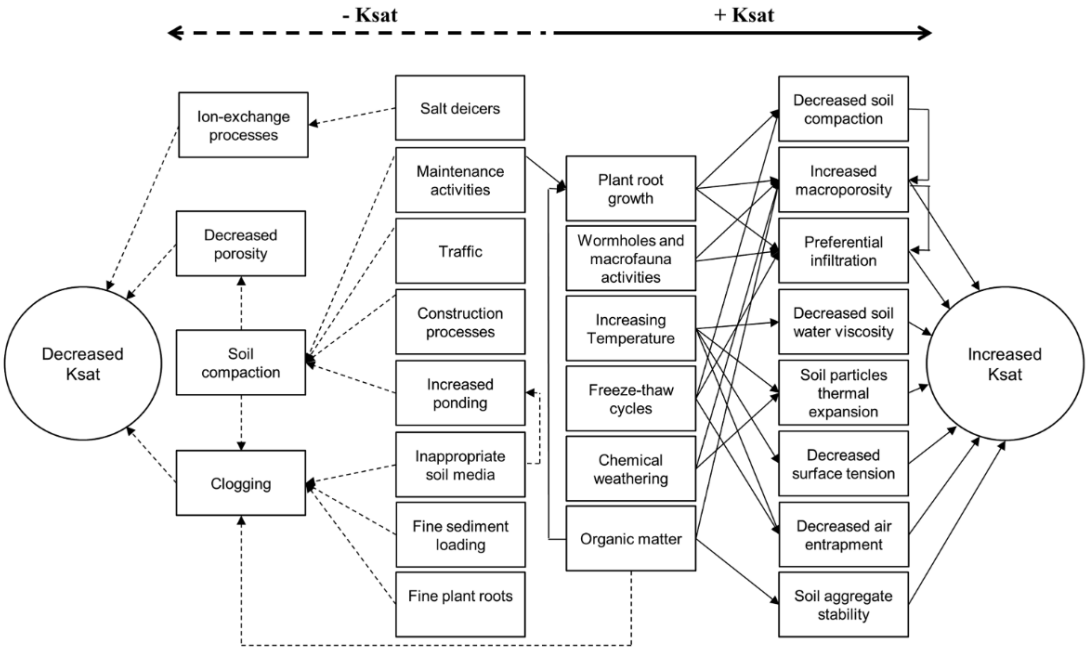

Figure 2.5: Causes of variability in field saturated hydraulic conductivity of SuDS (Ebrahimian et al., 2020)

2.2 Groundwater flow

Groundwater flow can be divided into two main zones: the saturated zone and the unsaturated zone. The unsaturated zone, also known as the vadose zone, is the area of soil located above the groundwater table, while the saturated zone lies beneath it, as illustrated Figure 2.1.

2.2.1 Unsaturated zone

The unsaturated zone is wetted by a lowering groundwater table (saturated soil becomes unsaturated) and through infiltration from rainfall which percolates through the unsaturated zone before reaching the groundwater table. Flow in the unsaturated zone has different characteristics compared to flow in the saturated zone. Here, the pores are partially filled with air, which influences the permeability and hydraulic conductivity of the soil. These depend on the wetness (water content) of the soil. The soil water content is influenced by the pore pressure or matric potential in the soil. In the unsaturated zone, the pore pressure is negative. The relationship between this suction and water content can be described by a water retention curve (WRC). Typical water retention curves for clayey, silty loam, and sandy soils are shown in Figure 2.6.

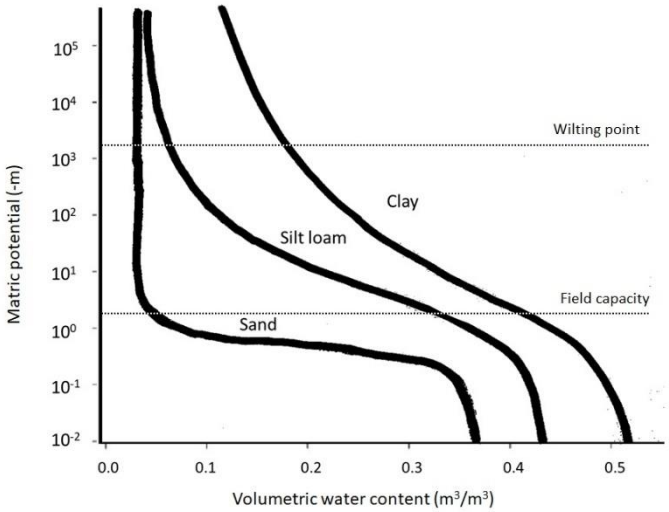

Figure 2.6: Soil water retention curves (Sela, 2024)

Water budget parameters related to the amount of water available for plant uptake can be visualised in the water retention curve (Figure 2.6). These include field capacity (FC), wilting point (WC) and plant available water (AW). Field capacity corresponds to a water content at which excess water has drained away and the downward movement of water has decreased. This usually takes place within 1-3 days after a rainfall or irrigation event (Assi et al., 2019). The corresponding suction depends on the soil type. For sandy soils, the soil is at field capacity at a pressure potential of -10kPa or (pF 2.0) (Gijsman et al., 2007). The permanent wilting point (PWP) is reached when plants can no longer extract water from the soil due to high matric forces. PWP is crop-specific and usually has a moisture potential of pF 4.2, which corresponds to a pressure potential of 1500 kPa (Gijsman et al., 2007). Plant-available water (AW) is defined as the difference between the moisture content at field capacity and the permanent wilting point (Assi et al., 2019).

Brooks and Corey (1964) and Van Genuchten (1980) formulated formulae to compute the soil water retention for different soil types.

Van Genuchten

Van Genuchten (1980) formulated an empirical equation for the water retention curve that relates moisture content (θ) to the soil suction (h) in the soil. This equation reads:

$$\theta = \theta_r + \frac{\theta_s - \theta_r}{(1 + |\alpha h|^n)^m}$$

where,

θ_r	=	residual water content (the water content for which the gradient ($d\theta/dh$) becomes zero ($cm^3\ cm^{-3}$)
θ_s	=	saturated soil water content ($cm^3\ cm^{-3}$)
α	=	empirical scale parameter: inversely proportional to mean pore diameter
n	=	empirical shape parameter: measure of pore-size distribution (-)
m	=	$1 - 1/n$

After combining this equation with the Mualem models (Mualem, 1976) an expression is obtained for the unsaturated hydraulic conductivity as a function of soil-water suction. First the effective saturation S_e can be computed as:

$$S_e = \frac{\theta(h) - \theta_r}{\theta_s - \theta_r}$$

With the use of the value for S_e at a certain suction *h* and the saturated hydraulic conductivity (K_s) the unsaturated hydraulic conductivity is described as follows (Schaap & Van Genuchten, 2006):

$$K = K_s * S_e^L \left(1 - \left(1 - S_e^{\frac{1}{m}}\right)^m\right)^2$$

Where L is an empirical connectivity parameter and a value of 0.5 is commonly used (Mualem, 1976).

Brooks and Corey

Brooks and Corey (1964) defined a similar expression to compute the water retention curve. This equation reads:

$$\frac{\theta - \theta_r}{\theta_s - \theta_r} = \left(\frac{h_b}{h}\right)^{\lambda}$$

where,

θ_r	=	residual water content ($cm^3\ cm^{-3}$)
θ_s	=	saturated water content ($cm^3\ cm^{-3}$)
λ	=	pore size distribution index (-)
h_b	=	air entry potential (kPa)

Brooks and Corey (1964) developed a similar equation where the relationship between the unsaturated hydraulic conductivity and moisture content is defined:

$$K(\theta) = K_s(S_e)^{\frac{(2+3\lambda)}{\lambda}}$$

where,

K_s	=	saturated hydraulic conductivity ($L\ T^{-1}$)
S_e	=	effective saturation (-)
λ	=	pore size distribution index (-)

Richards

Richards' equation (Richards, 1931) describes the flow of water in an unsaturated porous medium. The equation is highly non-linear (Niswonger et al., 2006). Therefore, the solution of this equation requires numerical solutions and is computationally expensive (Farthing & Ogden, 2017). The equation can be written in the vertical dimension as a function of the water content as follows:

$$\frac{\partial\theta}{\partial t} = \frac{\partial}{\partial z}\left(D(\theta)\frac{\partial\theta}{\partial z} - K(\theta)\right)$$

where,

θ	=	volumetric water content ($cm^3\ cm^{-3}$)
z	=	elevation in the vertical direction (positive downward (L)
$D(\theta)$	=	soil water diffusivity ($L^2\ T^{-1}$)
t	=	time (T)
$K(\theta)$	=	unsaturated hydraulic conductivity function ($L\ T^{-1}$)

2.2.2 Saturated zone

Flow in the saturated zone does not depend on soil moisture content as al pores are filled with water. Saturated flow can be calculated with the use of Darcy's law (Darcy, 1856, as cited in Brown, 2002). It shows an empirical, linear relationship between the discharge Q through the saturated soil and the drop in hydraulic head (Δh) over a distance L. Darcy's law is expressed as:

$$Q = kA\frac{\Delta h}{L}$$

where,

k	=	hydraulic conductivity of the soil (L T^{-1})
Q	=	discharge (L^3 T^{-1})
A	=	cross-sectional area perpendicular to the flow direction (L^2)
Δh	=	change in hydraulic head (L)
L	=	distance (L)

The hydraulic conductivity in Darcy's law reflects the relative ease of liquid flow through porous media. The hydraulic conductivity is a property of the soil and the fluid. The hydraulic conductivity can vary in different directions in the soil and can either be isotropic or anisotropic. Differences in the vertical direction can occur as different soil layers have different hydraulic properties, and in horizontal direction due to different soil composition and compaction.

2.2.3 Preferential flow

When discussing water flow in unsaturated soils, the presence of preferential flow paths cannot be ignored. According to Flury et al. (1994), preferential flow in the unsaturated zone is rather a rule than an exception. The unsaturated zone cannot be interpreted as homogenous and, consequently, water moves faster and in greater quantities at certain locations within the unsaturated zone compared to others (Hendrickx & Flury, 2001), bypassing large parts of the soil matrix.

Preferential flow can be classified into three main types: macropore flow, funnelled flow, and fingered flow (Stumpp & Kammerer, 2022). Macropore flow involves water movement through root channels, earthworm burrows, and soil cracks (Hendrickx & Flury, 2001). In bioswales, macropore flow is expected to have the greatest impact on performance compared to other types of preferential flow. For instance, Bockhorn et al. (2017) found that infiltration increased by 61% when earthworm burrows were present in the soil.

Water bypasses the denser, less-permeable soil matrix by taking the path of least resistance through macropores. These macropores become hydraulically active when soil matric potential exceeds the water entry potential of the macropores, but they do not conduct water in relatively dry soils (Bockhorn et al., 2017). Several modelling approaches exist to account for macropore flow in unsaturated soils. One such approach is the dual-domain model, which divides the soil into two domains: the soil matrix and the macropore system (Guertault & Fox, 2020). Ghasemizade (2015) explored three conceptual models of increasing complexity to represent macropore flow (see Figure 2.7). In the model simulating homogeneous matrix flow (a, in Figure 2.7), a higher hydraulic conductivity was used to represent the rapid flow due to macropores. In the dual-permeability model (b, in Figure 2.7), additional parameters were introduced, with different hydraulic conductivities assigned to the matrix and macropores. The third model (c, in Figure 2.7) added further complexity by incorporating vertical heterogeneity.

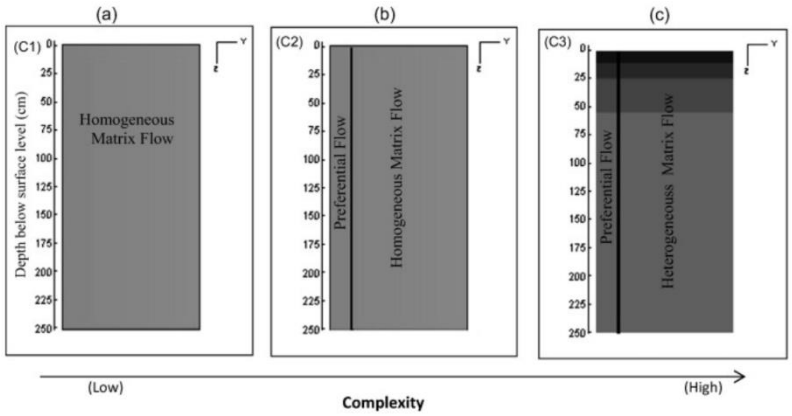

Figure 2.7: Conceptual groundwater models with various levels of complexity in a vertical cross-section (Ghasemizade, 2015)

Regardless of the type of preferential flow, it remains challenging to measure, quantify, and predict water flows due to their complexity, especially when looking at the interaction between matrix water content and macropore flow (Nimmo, 2021).

3. Methodology

This chapter describes the bioswale groundwater model and methodology used during the research.

3.1 Bioswale groundwater model

This section describes the conceptualisation of hydrological processes in the bioswale groundwater model developed by Deltares, followed by an explanation of model-specific parameters and a description of the main equations in the model to represent unsaturated zone flow. The set-up of the model for the specific case-study area is described in section 4.3.

3.1.1 Modelling concept

The functioning of bioswales is modelled using a physical approach that describes the hydrological processes, relying on equations derived from principles of soil physics. The processes of rainfall, infiltration and percolation within the subsoil are conceptualised in the provided model. Figure 3.1 illustrates these interactions.

Figure 3.1 illustrates the conceptualisation of the bioswale groundwater model in three stages. Water from rainfall and runoff from surrounding areas can pond on the surface and enters the ‘ponding bucket’. The size and shape of this bucket depend on surface level grid input. Rainfall that does not result in runoff to the bioswale infiltrates locally and results in groundwater recharge directly (with the Recharge package of MODFLOW).

Next, the ponded water infiltrates into the unsaturated zone and as a result the water level in the bioswale (the ‘ponding bucket’) decreases with every timestep. Unsaturated zone flow is simulated as vertical flow with the Unsaturated Zone Flow (UZF) package of MODFLOW. Flow in the unsaturated zone relies on predefined parameters such as moisture content and hydraulic conductivity for different soil layers. Soil layers can be specified within the bioswale with a specified thickness and are referenced to the surface level grid. Horizontal variations in hydraulic conductivity can be made to represent different soil types within the bioswale.

Subsequently, the water flows into the saturated zone, where 3D simulations of flows are calculated using MODFLOW 6. Water enters the drain that is conceptualised with the River package of MODFLOW. The grid cells of the drain are assigned a conductance that relates the difference in head to the rate of flow. The sum of the outflow in these grid cells represents the discharge through the drain. With this model conceptualisation, the water level in the bioswale, groundwater heads in the bioswale and the surroundings and drain discharges can be computed.

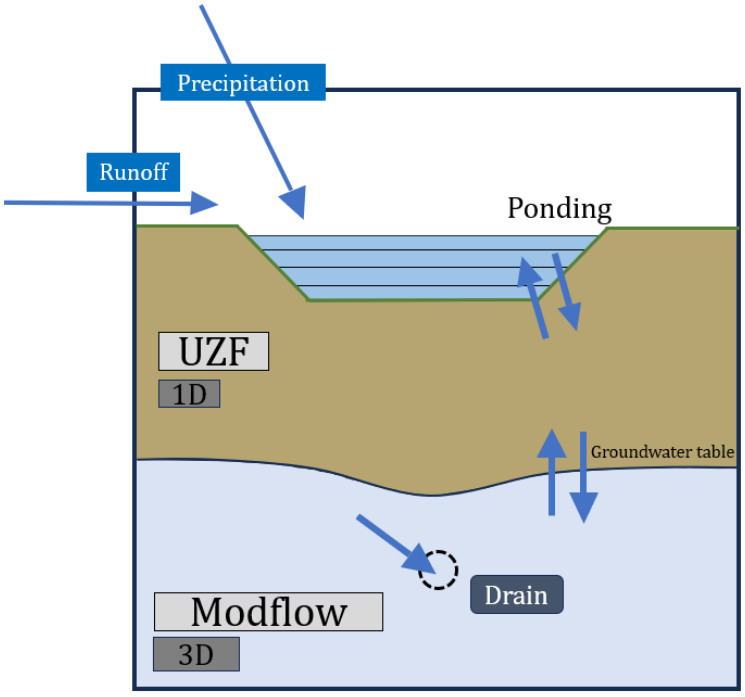

Figure 3.1: Schematization of bioswale groundwater model

The conceptualisation of hydrological processes in the current bioswale groundwater model has certain limitations and assumptions that need to be addressed. These can be identified as follows:

- Since soil layers are defined relative to the ground level, the drain (which has an absolute, not a relative, depth) may intersect multiple soil layers. This effect is most notable at the sides of the bioswale, where the ground level is higher, causing the drain to be placed in a model layer beneath the intended drainage layer.

- The bioswale groundwater model does not include a routing aspect, meaning the travel time of runoff to the bioswale is not incorporated.

- Water entering the bioswale is collected in the lowest point of the bioswale before it starts infiltrating.

- The drain is conceptualised using the input grid-cells, meaning that calculations of flow within the drainage pipe is not included in this model. As a result, energy losses and the difference between the flow in partially and fully filled drains are not considered.

- The hydraulic conductivity values can be specified in horizontal and vertical direction. Other soil parameters such as residual moisture content and specific yield can only be specified in vertical direction for different soil layers, but no horizontal differentiation can be made.

3.1.2 Model parameters

The bioswale groundwater model has different (soil) parameters to describe the unsaturated zone flow and the working of a bioswale. In Appendix A an overview can be found of all the model parameters. This paragraph will describe the model parameters that are specific for this bioswale groundwater model. The soil parameters used by the UZF-package, such as hydraulic conductivity, Brooks-Corey epsilon and moisture content, are typical groundwater parameters and will not be discussed in detail.

The infiltration rate of the ponding water in the soil depends on the infiltration parameter of the bioswale I_{swale} (m/d) and the bottom conductance of the bioswale C_{bottom} (d). This is described in the following formula:

$$Infiltration\ rate = \min\left(I_{swale} + \frac{Water\ level}{C_{bottom}},\ K_{s,top}\right)$$

The I_{swale} parameter is a characteristic of the bottom of the bioswale. It represents the turf layer that can have different infiltration characteristics compared to the direct soil layer underneath, due to leaves, holes and vegetation type. The infiltration into the unsaturated zone depends on the relation between the vertical hydraulic conductivity of the topsoil layer ($K_{s,top}$) and the I_{swale} parameter. When the I_{swale} parameter is smaller than $K_{s,top}$, I_{swale} becomes the controlling parameter for infiltration. However, when $K_{s,top}$ is smaller, this parameter will control infiltration into the unsaturated zone.

The C_{bottom} parameter determines the head-depended infiltration of the soil, relating a higher water level in the bioswale to faster infiltration.

The drain is represented by grid cells that each have a total conductance $C_{drn,total}$ (m^2d^{-1}). Grid cells further away from the specified drain location get a lower conductance and grid cells that cross the drain get a higher conductance, depending on de specified drain parameters. The total conductance of the drain depends on the entry resistance of the drain (C_{drn}) (d) and the width of the drain (W_{drn}) (m). The width of the drain does not correspond to the actual drain width that is usually smaller than the grid cell size. The entry resistance of the drain depends on the drain diameter, distribution of fill material, the amount of clogging and the number and sizes of drain openings. As detailed information about these aspects is usually unknown, C_{drn} is usually determined during model calibration (Harbaugh, 2005).

3.1.3 MODFLOW and UZF

MODFLOW is a finite difference groundwater model developed by the United States Geological Survey (USGS). It computes groundwater flows in three dimensions based on pre-defined grid cells in horizontal and vertical direction (Harbaugh, 2005) (see Figure 3.2).

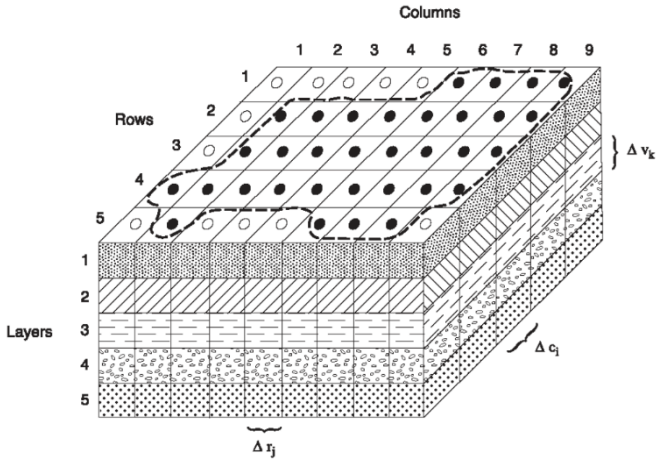

Figure 3.2: Schematization of MODFLOW grid cells (Harbaugh, 2005)

MODFLOW includes an Unsaturated-Zone Flow package (UZF), which computes groundwater flows in the unsaturated zone in the vertical dimension. The Richards equation, as described in section 2.2.1, is approximated in the UZF package with kinematic waves (Niswonger et al., 2006). The moisture content wave moves downward through the soil as infiltration continues. It is assumed

that vertical flux is only driven by gravitational forces. This leads to a simplified Richards equation, where the diffusive term, $D(\theta)\frac{\partial\theta}{\partial z}$, is neglected (Niswonger et al., 2006):

$$\frac{\partial\theta}{\partial t} + \frac{\partial K(\theta)}{\partial\theta}\frac{\partial\theta}{\partial z} + i = 0$$

The Brooks-Corey function (described in section 2.2.1) is used in the UZF package to compute unsaturated hydraulic conductivity. The exponent $\frac{(2+3\lambda)}{\lambda}$ is referred to as the Brooks-Corey exponent and the parameter EPS is used in the UZF package for this exponent (Niswonger et al, 2006). This parameter will be referred to with ε in the remainder of this thesis.

The simplifications in the UZF package regarding unsaturated zone flow lead to the exclusion of two key hydrological processes:

- Capillary rise is not modelled. This is because diffusive term in the Richards equation is neglected. Evaporation and uptake by roots can cause water to flow upward. Neglecting this process can result in an underestimation of water available in the rootzone and an overestimation of groundwater recharge. This is acceptable in the context of modelling bioswale response as the focus is on downward infiltration and drainage, where gravitational forces are dominant.

- The influence of preferential flow in the unsaturated zone is excluded. This is because the UZF package assumes the unsaturated zone is homogeneous. This can lead to an underestimation of unsaturated fluxes of water, which is often present in hydrological models (Mirus & Nimmo, 2013). This can result in a time-lag between modelled and observed discharges. By incorporating measurement data, this time-lag can be quantified and key processes such as infiltration and drainage can still be modelled, thereby justifying the assumption of a homogenous unsaturated zone in the UZF package.

3.2 Model calibration

The bioswale groundwater model was calibrated to obtain model parameter values that are hard to measure or estimate. The measurement data was split into a calibration and validation datasets. With the obtained parameter set from calibration, the model was validated with new, unseen, data and the performance of the model could be assessed.

The model was calibrated using a Monte Carlo approach: samples were drawn for every calibration parameter between the predefined minimum and maximum values. For every parameter combination, the modelled output was compared to the measurements. Objective functions shown below were then used to assess the goodness of fit of the model and the optimal parameter values were selected. Monte Carlo calibration assumes that model parameters are independent. However, as described in Section 3.1.2, the parameters I_{swale} and $K_{s,top}$ are not independent. To account for this, a constraint was applied during calibration, ensuring that I_{swale} is always equal to or smaller than $K_{s,top}$. Other parameters, such as hydraulic conductivity and Brooks-Corey epsilon, may have physical relationships, but these are harder to describe with constraints. Therefore, they were treated as independent here to simplify the calibration process.

3.2.1 Calibration parameters

The selected model parameters that were calibrated are shown in Table 3.1, together with the corresponding calibration ranges. These model parameters were selected because they were found to influence model output the most when adjusting them manually. Additionally, they play key roles in controlling important hydrological processes in the model, such as infiltration, drainage,

and unsaturated flow, while specific values for these parameters could not be obtained from literature or measurements.

Table 3.1: Parameter ranges used for calibration of the bioswale groundwater model

Parameter	Description	Minimum	Maximum
$K_{s,\ top}$	Saturated hydraulic conductivity top layer (m/d)	0.1	20
$K_{s,\ sand}$	Saturated hydraulic conductivity sand layer (m/d)	0.1	20
ε_{top}	Brooks Corey Epsilon top layer (EPS) (-)	3.5	6
ε_{sand}	Brooks Corey Epsilon sand layer (EPS) (-)	3.5	6
$C_{drn,\ factor}$	Drain conductance factor (-)	0.001	1
I_{swale}	Infiltration parameter (m/d)	0.05	2
C_{bottom}	Bottom conductance (d)	0.1	10

The saturated hydraulic conductivity (K_s) was varied for the topsoil of the bioswale and the sand layer where the drain is located. The hydraulic conductivity of the native soil surrounding the improved bioswale layers was not calibrated, based on the assumption that water infiltration and percolation occur within the improved soil layers, as intended by the bioswale design. The soil layers were assumed to be isotropic, meaning vertical and horizontal hydraulic conductivity were assumed to be equal.

The Municipality of Rotterdam typically designs bioswales with a soil texture hydraulic conductivity between 0.3 and 0.5 m/d. These values are also recommended by Boogaard et al. (2006). A higher maximum value for the hydraulic conductivity (20 m/d) was used during calibration to account for preferential flow in the unsaturated zone, as recommended by Ghasemizade et al. (2015) and Ahmed et all. (2015). These studies observed higher hydraulic conductivities in bioswale-like structures than was expected from the textural soil classes. A minimum value slightly lower than 0.3 m/d (0.1 m/d) was used during calibration.

The Brooks-Corey exponent (ε) relates the water content to unsaturated hydraulic conductivity. The minimum value of ε was set to 3.5 as this is the minimum and default value in the UZF-package. A higher maximum bound was set as a maximum for both layers to include for more heterogeneity in the soil (Vereecken et al., 2019). A maximum value of 6 was used as this value for ε corresponds to a value for lambda in the Brooks-Corey equation of 0.6 for sandy soils in Hydrus 1D.

Multiple parameters determine the total drain conductance of the drain. It was decided to change the total conductance of the drain by multiplying the total conductance with a multiplication factor of a value between 0.001 and 1. This corresponds to a range in entry resistance of the drain between 0.1 and 10 days.

The range used for the infiltration parameter was based on measurements of infiltration rates in bioswales. The experiments by Mobron (2019) and students of Hanzehogeschool Groningen (Goede, 2022) resulted in infiltration rates in bioswales in Rotterdam corresponding to values for the infiltration parameter within these defined ranges.

As there are no measurements or values from literature available that represent the bottom conductance parameter of the bioswale groundwater model, a wide range between 0.1 and 10 days was used.

3.2.2 Sampling

Samples were drawn for each parameter between the ranges defined in Table 3.1, assuming a uniform distribution for all calibration parameters. This approach considers all values within the range equally probable. Due to the model's runtime constraints, the Monte Carlo calibration was

limited to 150 samples. Given the small sample size, Latin Hypercube Sampling (LHS) was chosen over random sampling. In LHS, the range of each parameter is stratified into 150 equal, uniformly distributed intervals, from which one sample is randomly selected per interval. This approach ensures faster convergence, and a more equal distribution of samples compared to random sampling. This is illustrated in Figure 3.3, where the improved sampling convergence using LHS is shown.

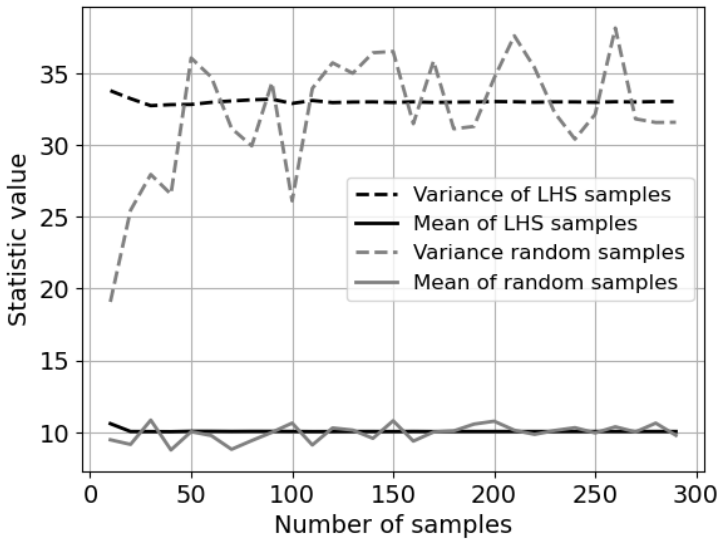

Figure 3.3: Sampling convergence for random sampling versus LHS sampling

3.2.3 Objective functions

Three different objective functions were used to evaluate the goodness of fit between the model outputs and the corresponding measurements. The Nash-Sutcliffe Efficiency Index (NSE) (Nash & Sutcliffe, 1970) is commonly used to assess the accuracy of hydrological models (Haghighatafshar et al., 2019; Zhang & Chui, 2022). The formula is as follows:

$$NSE = 1 - \frac{\sum_{i=1}^{n}\left(y_o^i - y_m^i\right)^2}{\sum_{i=1}^{n}\left(y_o^i - \bar{y}_0\right)^2}$$

Here, $\bar{y}_0$ represents the mean of the observed variable, y_m^i is the modelled result at time i and y_o^i is the value of the observed variable at time i. An NSE of 1 indicates a perfect fit between the model output and observations, while an NSE of 0 means that the model performs equally well as the mean values of the observations (Jain & Sudheer, 2008). According to Jain & Sudheer (2008) it is not advisable to conclude the performance of a model purely on the NSE index as it can be sensitive to bias and peak values. Therefore, the normalised Root Mean Squared Error (NRMSE) and the Mean Absolute Percentage Error (MAPE) were used as objective functions as well.

$$NRMSE = \frac{\sqrt{\frac{1}{n}\sum_{i=1}^{n}(y_o^i - y_m^i)^2}}{y_{m,max} - y_{m,min}}$$

The NRSME normalises the RMSE values by the difference between the minimum and maximum model results, making the objective function scale invariant. However, NRMSE is sensitive to large errors as it squares the difference between modelled results and observations. Unlike NRMSE, MAPE treats all errors equally in relative terms by dividing the difference by the observed values:

$$MAPE = \frac{1}{n}\sum_{i=1}^{n}\left|\frac{y_o^i - y_m^i}{y_o^i}\right| * 100\ \%$$

To combine the objective functions of multiple measured hydrological variables (such as drain discharge and water level), a weighted sum approach was used. Equal weights were assigned to the objective functions of the different hydrological variables, resulting in a total optimal parameter set.

Due to the missing of preferential flow processes in the bioswale groundwater model, there can be a time-lag between the modelled and observed arrival times, resulting in poor objective function results. Therefore, the discharge output graph was shifted to align with the moment a reaction is observed in the drain during the measurements. In this way, the discharge output in the drain was calibrated purely on the shape of the curve, not on the arrival time.

3.3 Sensitivity analysis

After calibrating and validating the model, a sensitivity analysis was performed to evaluate the influence of different factors on the performance of bioswales. The sensitivity analysis focused on two main functional requirements: peak discharge and emptying time. From the performance criteria described in section 2.1.2, these two performance requirements are defined as the most important design criteria for urban drainage systems by the experts of the municipality of Rotterdam. The peak discharge and emptying time were calculated based on the instant filling of the bioswale. Additionally, the analysis evaluated the model's sensitivity to the time-lag observed in the modelled drain discharges.

A *one-at-a-time* (OAT) sensitivity analysis (Lenhart et al., 2002) was conducted on the calibration parameters. The optimal parameter set obtained from model calibration was adjusted one parameter at a time while keeping the other parameters constant. The variations ranged from -90% to +90% in steps of 15%. The minimum value for the ε parameter is 3.5, as this is the default and minimum value for this parameter in the UZF package. By changing the parameters linearly in positive and negative directions, nonlinear model responses can be identified. It is important to note that this approach is a local sensitivity analysis, where parameters are assumed to be independent of each other. Although some parameters may be physically related, treating them as independent simplifies the analysis and provides insight into their individual contributions to the modelled output.

With these parameter ranges, peak outflow discharge, emptying time, and time-lag between modelled drain discharge and measurements were computed. The unsaturated hydraulic conductivity, which depends on the soil moisture content as described by the Brooks-Corey equation in the UZF package (see section 3.1.3), also influences the time-lag in the model. Therefore, the sensitivity of the model to maximum moisture content during percolation in the middle of the top layer was also evaluated.

To assess the effect of antecedent moisture content on the time-lag in the model, higher moisture content levels were simulated by increasing the residual moisture content (θ_r) of the top layer. Since this parameter was not part of the calibration process, θ_r was modified separately.

3.4 Bioswale performance assessment

The methodology for assessing bioswale performance is explained in this section. The performance is evaluated under various weather and climate conditions whilst considering different bioswale designs.

3.4.1 Weather and climate scenario analysis

To evaluate the performance of bioswales in Rotterdam, new scenarios were created that test the bioswales in summer and winter under current and future climate conditions. The differences in the hydrological response of bioswales between these two seasons were captured in model parameters and characteristic design storms. Figure 3.4 shows a diagram of the different weather and climate scenarios analysed here, which will be explained further below. The performance under individual design storms was assessed based on the following performance criteria (see section 2.1.2): emptying time, maximum water depth and peak outflow discharge. With the rainfall data, the maximum ponding duration criterion could be assessed as well.

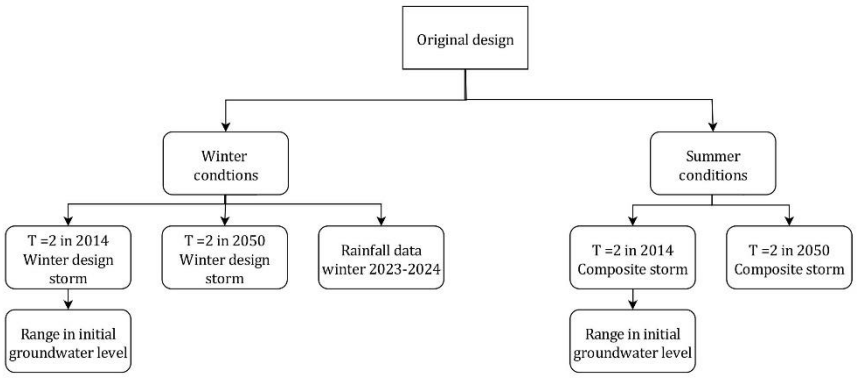

Figure 3.4: Diagram of tested weather and climate scenarios

Design storms

To evaluate the performance of bioswales, storms designed to represent winter and summer rainfall events were developed for current and future climates. These design storms are based on weather statistics from the *Foundation for Applied Water Research* (STOWA, in Dutch: *Stichting Toegepast Onderzoek Waterbeheer*) and climate scenarios from the *Royal Netherlands Meteorological Institute* (KNMI, in Dutch: Koninklijk Nederlands Meteorologisch Instituut).

Composite storms from RIONED were used to test the performance of bioswales under a peak rainfall event in summer, as such events are expected to become more frequent during that season. According to the bioswale guidelines of the municipality of Rotterdam, a bioswale is allowed to spill over during a rainfall event with a return period of two years (Mobron, 2024). Since the expected lifespan of a bioswale in Rotterdam is about 50 years, it must still meet performance criteria under the 2050 climate scenario, around halfway of the bioswale's lifetime (Mobron, 2024). The wettest climate scenario (Wh) (KNMI, 2015) was selected for the composite storm in 2050. The composite storms from RIONED used to test the bioswales under a heavy summer rainfall event, are shown below in Figure 3.5.

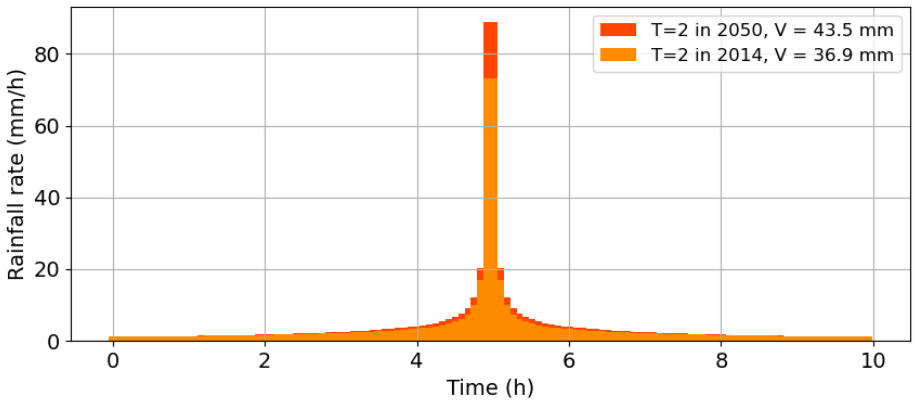

Figure 3.5: Design storms for heavy summer rainfall events (RIONED)

The performance of bioswales is expected to be different under summer and winter conditions. Therefore, a longer and lower peak design storm characteristic for the winter has been computed (see Figure 3.6). These were computed based on the method described by Vaes & Berlamont (1996), making use of STOWA (Beersma et al., 2019) and KNMI (KNMI, 2023) statistics. The winter design storm has a longer duration (48 hours), and lower peak compared to the composite storm from RIONED in Figure 3.5 used for the summer. This simulates the typical longer duration, higher volume, and lower intensity rainfall events seen in winter. The KNMI reported an expected 7% increase in total rainfall in winter by 2050 in the wettest scenario (KNMI, 2023). Since the increase is expected to be primarily in total volume rather than peak intensity, the 2014-based design storm was multiplied by this 7% to create a winter rainfall design storm expected for a two-year return period in 2050.

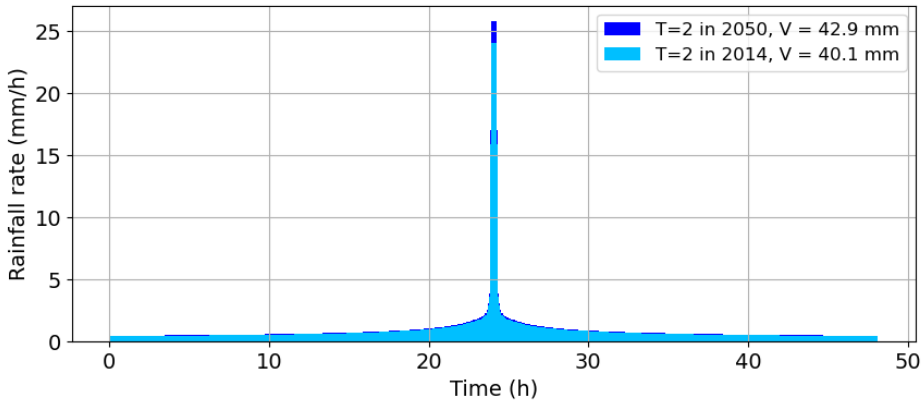

Figure 3.6: Computed design storms for winter rainfall events

Rainfall data

During winter and wetter periods, consecutive rainfall events can cause bioswales to flood or retain water for extended periods. These multiple rainfall events are not represented by the composite storms of Figure 3.6. Therefore, rainfall data was used to evaluate the performance of bioswales under consecutive rainfall events. The period of November 2023 to February 2024 was selected as this was a relatively wet period, with 50% more rainfall than an average winter (KNMI, 2024).

As described in Appendix D, three different rainfall measurement sources are available in Rotterdam. As rainfall station data is missing for the beginning of November 2023 and due to its higher resolution of 15 minutes compared to the KNMI's hourly measurements, radar data from the Delftse Poort was used to evaluate bioswale performance during a wet winter. The selected rainfall intensity data from the radar are presented below in Figure 3.7.

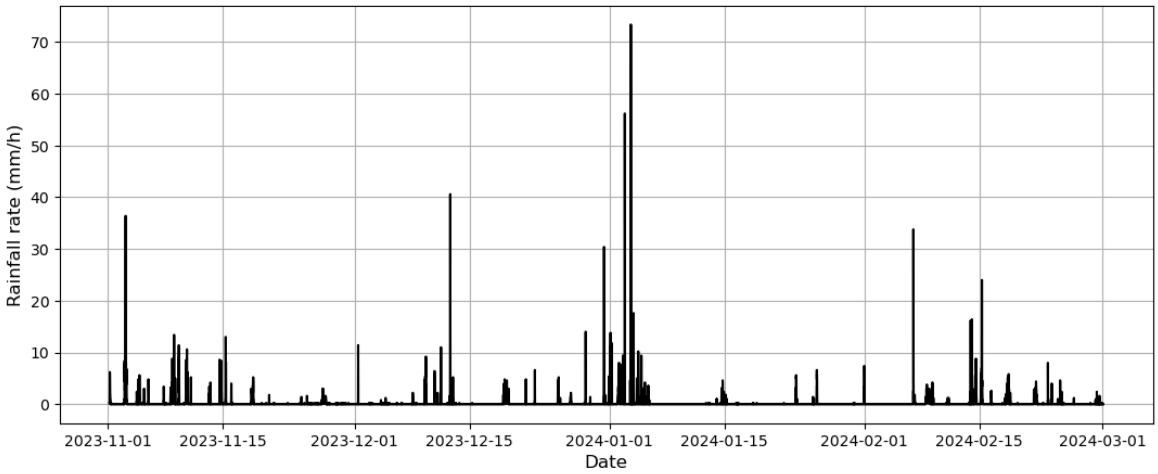

Figure 3.7: Radar (Delftse Poort) rainfall data from November 2023 – February 2024

Summer and winter conditions

Not only do rainfall duration and intensity differ between winter and summer, but other factors, such as temperature and vegetation, also change with the seasons. As a result, parameters in the bioswale groundwater model must be adjusted when simulating different seasons. This section discusses how variations in infiltration rate, hydraulic conductivity, groundwater levels, and evaporation were accounted for in modelling bioswale performance for the two seasons.

Infiltration rate

The infiltration rate of bioswales can vary between seasons due to factors such as biological activity, vegetation development, and temperature (see section 2.1.3). The I_{swale} parameter determines the rate of infiltration and was calibrated based on measurements at the end of winter in 2019. Therefore, the I_{swale} parameter was adjusted based on measurements during summer-like conditions of the case-study bioswale conducted by students of Hanzehogeschool Groningen (Goede, 2022). The analysis of the results of the measurements is described in Appendix E. This results in different values for I_{swale} during summer and winter conditions, presented in Appendix G.

Hydraulic conductivity

As described in section 2.1.3. the hydraulic conductivity changes with temperature as a result of the relation between the viscosity of water and temperature. To simulate winter conditions, the calibrated hydraulic conductivities were used as these were calibrated on measurements from February to March 2019. Between 5 and 20 degrees Celsius the viscosity increases by 50%, therefore the hydraulic conductivities used to simulate summer conditions are 50 % higher than in winter conditions.

Groundwater levels

Groundwater levels in the gardens can fluctuate due to water uptake by roots and adjustments made by the waterboard to the set drainage level. When the drain is connected to surface waters, the groundwater level at the drain location can be kept constant during drier periods, keeping the drain submerged. However, when the drain is not connected to surface waters, the groundwater level can drop below the depth of the drain. This response was not evaluated during the model parameter sensitivity analysis, and therefore evaluated in these scenarios.

To assess the effect of a lower and higher groundwater table, minimum and maximum ranges have been identified from groundwater measurements from piezometers in surrounding gardens (see Appendix F). These same ranges were applied for both winter and summer scenarios to allow for a comparison of the results. In further model scenario simulations, the set drainage level in the area was used as the initial groundwater level.

Evaporation

Water loss due to evapotranspiration and open water evaporation is expected to vary between summer and winter because of differences in temperature, sunlight hours, and wind. To estimate the magnitude of this difference, evapotranspiration and open-water evaporation have been roughly calculated. Open water evaporation was determined using the Penman-Monteith equation (Penman, 1948). The data for the various parameters in the equation were obtained from measurements at the KNMI weather station in Zestienhoven. The average open water evaporation during the summer (June, July and August) was calculated to be 5.5 mm per day.

The KNMI provides Makkink evapotranspiration data using grass as a reference vegetation. The average evapotranspiration for the summer months was calculated to be 3.2 mm per day. These values are consistent with the order of magnitude reported by KNMI.

These evaporation values are relatively small compared to the size and volume of the design storms used. Additionally, studies examining the effect of temperature on hydraulic conductivity have shown that evapotranspiration is often insignificant compared to the rate of infiltration (Emerson & Traver, 2008). For these reasons, the impact of evaporation on the performance of bioswales in the different seasons has not been included in the remainder of the study.

Determining connected paved surface
To evaluate the performance of bioswales, bioswales should be filled with water during a design storm with a return period of two years. When designing bioswales, the water depth in the bioswale may not exceed 30 cm (see section 2.1.2.) during this design storm. Based on this criterion, the potential connected paved surface area can be computed. The potential connected paved surface was calculated based on the surface area that would cause the water depth to reach 30 cm during the T=2 design storm of 2014 in summer. The runoff area from rainfall falling in nearby gardens and flowing with a small slope to the bioswale was incorporated with a runoff coefficient of 0.3. This area was determined from the DTM using QGIS. The remaining paved surface that can be connected was incorporated with a runoff coefficient of 0.8. The obtained runoff area for the specific case-study bioswale is presented in Appendix G.

3.4.2 Design scenario analysis

Two different design scenarios were analysed and their performance regarding emptying time and peak discharge was evaluated. These are as follows:

Scenario A: Drain location and sand type
The bioswale drain was placed further away from the original location (in the centre of the case-study bioswale). It was expected that this will increase the distance to the drain and therefore reduce the peak flow. Furthermore, different sand types used for constructing the bioswale were evaluated as well.

Scenario B: Increased bottom width of bioswale
To evaluate the effect of a wider bottom of the bioswale in combination with constructing two drains, the design of the original case-study bioswale was modified. The amount and distance between drains were evaluated for a wider bioswale and the sand type was varied as well.

Design scenario A: Drain location and sand type
The performance was tested in the most critical situation, using the composite storm of T=2 in 2050, in combination with different drain locations and sand types. The performance was evaluated based on peak discharge and emptying time. Figure 3.8 presents an overview of the scenarios analysed.

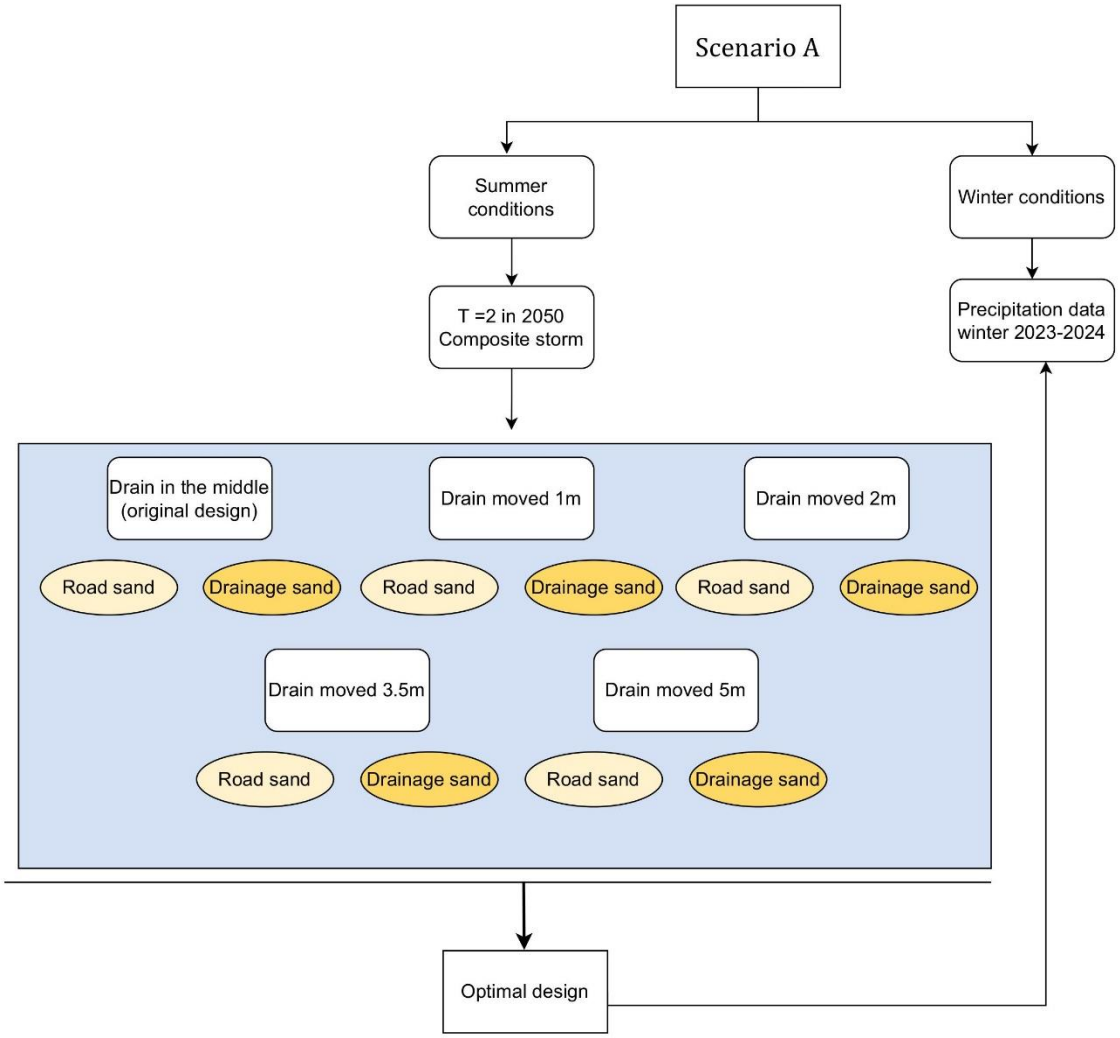

Figure 3.8: Overview design scenario A

The original drain location is in the centre of the bioswale, below the lowest point of the bioswale. The drain was relocated parallel to the original position in the horizontal direction, with distances ranging from 1 meter to 5 meters. As the water must travel a longer distance, a lower peak discharge is expected with increasing drain distance. Additionally, the sand layer promoting drainage was widened to ensure the water can reach the drain. A cross-section of the modified design of the case-study bioswale can be found in the results section (Figure 5.16).

The effect of sand type was evaluated as well. Two different sand types are used in the construction of bioswales in Rotterdam: road sand and drainage sand. Road sand is used as a foundation layer for road construction and consists of a mixed grain size distribution, ranging from fine to coarse, and may also contain silt. Drainage sand has a more uniform, coarser grain size distribution to facilitate drainage. Based on the analysis of predicted hydraulic conductivities derived from soil texture measurements of road sand by the Municipality of Rotterdam, a range between 1 and 3 m/d was used to model the effect of road sand. Drainage sand, with a coarser grain size distribution, typically corresponds to a hydraulic conductivity of 30 m/d according to Bot (2011). However, as the sand is expected to compact during construction and use of the bioswale (Ahmed et al., 2015), a conservative value range of 10 to 15 m/d was used for the hydraulic conductivity of drainage sand.

From the changes in drain distances and sand types, a new optimal design can be proposed that meets both the emptying time and peak discharge criteria. This new design was tested with the winter rainfall data described in section 3.4.1 (see Figure 3.7).

Design scenario B: Increased bottom width of bioswale

The Municipality of Rotterdam can decide to use two or more drains instead of one (Mobron, 2024). This is typically done when the bioswale is designed to be larger and more drainage capacity is needed. The distance between these two drains can affect both the emptying time and peak discharge as a result of the bulging of the groundwater level between the two drains and the distance the water must travel to reach them. To evaluate the effect of the distances between two drains, a wide bioswale with a bottom width of five meters was created (see Figure 5.20 in section 5.3.2). The top and sand layers were also designed with a width of 5 meters. The performance of this wider bioswale was tested with the design storm expected in 2050 with a return period of two years. Different distances between the two drains vary from 1 to 5 meters, in combination with the use of road or drainage sand. The modelled scenarios are illustrated in Figure 3.9 below.

Figure 3.9 Overview of design scenario B

As the volume of the bioswale increased by widening the bottom, an additional paved surface was connected to the runoff area, ensuring the bioswale reaches its full capacity (30 cm water depth) during the summer design storm with a two-year return period in 2014.

4. Case Study

This chapter introduces the real-life bioswale in Rotterdam that was analysed in this study, including the related measurement data and specifics of setting up the bioswale groundwater model presented in the previous chapter.

4.1 Description

Mobron (2019) conducted measurements at four different bioswales in the Zenobuurt in the Lombardijen district in Rotterdam. For this research, Wadi A from Mobron's study was selected as the case-study bioswale, as these measurements were the most complete compared to the measurements of the other bioswales. Bioswale A, located next to Plotinusstraat in the Zenobuurt, was constructed in 2017 (see Figure 4.1). The bottom of the bioswale has a depth of -2.1 m NAP, while the surrounding gardens are at -1.6 m NAP.

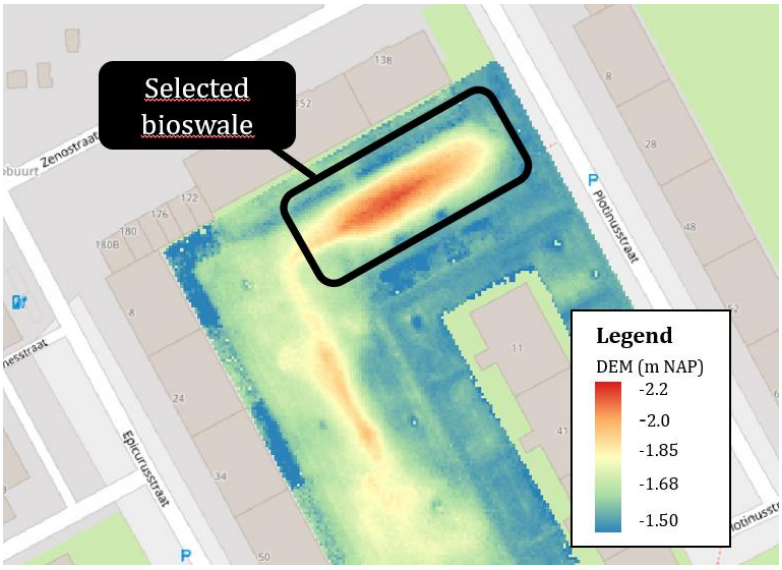

Figure 4.1: Location and inundation of the selected case-study bioswale

The bioswale's bottom layer was improved to a width of two meters, and the side slopes have the same soil as the garden's topsoil, based on Mobron's soil measurements. The drain is located in a sand bed constructed with drainage sand. A photo taken during the construction of the case-study bioswale (see Figure 4.2 below) shows the drain's location within the sand bed, surrounded by clay.

Figure 4.2: Photo taken during construction of the case-study bioswale

The drain is connected to the DIT-sewer (Drainage Infiltration Transport) and should maintain the set drainage level of -2.4 m NAP. Unlike Rotterdam's design guidelines for bioswales, there is no paved surface such as roofs or streets connected to this case-study bioswale, and it does not feature an outlet system for handling heavy rainfall events when water depths exceed 30 cm.

As can be seen in Figure 4.1, there is also an inundation in the gardens parallel to the Epicurusstraat, which was intended to function as a bioswale. However, since the top layer was not improved and Mobron's measurements showed no water flow to this area, the selected bioswale in Figure 4.1 was considered a bioswale on its own for this research.

4.2 Measurements

4.2.1 Storm simulations

Mobron (2019) assessed the performance of the bioswales through full-scale tests. Each bioswale was filled with a specified volume of water, and measurements were taken for outflow discharge, groundwater levels, and water levels. Four distinct 'storm' scenarios were simulated to represent various rainfall events:

- Storm 1: Heavy storm in dry initial conditions
- Storm 2: Heavy storm in wet initial conditions
- Storm 3: Two-peak storm
- Storm 4: Medium storm with longer duration

The antecedent moisture contents before the four storm simulations were not measured, so the exact initial moisture conditions for the full-scale tests remain unknown. However, Mobron (2019) suggested that storms 1, 3, and 4 were conducted under field capacity-like conditions, and storm 2 was performed in wetter initial conditions as this test was performed shortly after a rainfall event or another full-scale test.

Storms 1 and 2 each lasted about one hour, with the swale filled with approximately 30 m^3 of water. Storm 3 was filled twice: first with 20 m^3 of water, followed by 10 m^3. Storm 4 had a duration twice as long as the others but with less than half the inflow volume compared to storms 1, 2, and 3. The inflow volumes from the full-scale tests were converted to mm/day and used as rainfall input in the bioswale groundwater model.

4.2.2 Measurement data

Discharge was measured by Mobron (2019) in the manhole connected to the bioswale's drain with the use of a tipping bucket of three litres. By using a tipping bucket, high flow conditions may cause water to splash out of the bucket, potentially leading to an underestimation of discharge. The discharge data was smoothed using a moving window for comparison with the model output.

The surface water level during infiltration of the bioswale was measured with divers. Two divers were placed in the bioswale, their locations can be seen in Figure 4.3. However, the second diver's data was lost during Storms 2 and 3. For these storms, data is available only from a diver positioned 6.29 cm below the bioswale's lowest point (Mobron, 2019). The measured surface water level data was converted to m NAP and corrected with + 0.063 m if needed to be able to compare with the model output.

Groundwater levels were measured with level sticks and corrected for air pressure (Mobron, 2019). Five piezometers were installed at different distances from the drain and throughout the bioswale.

The locations of these five piezometers are presented in Figure 4.3, with the piezometers indicated with A1 – A5.

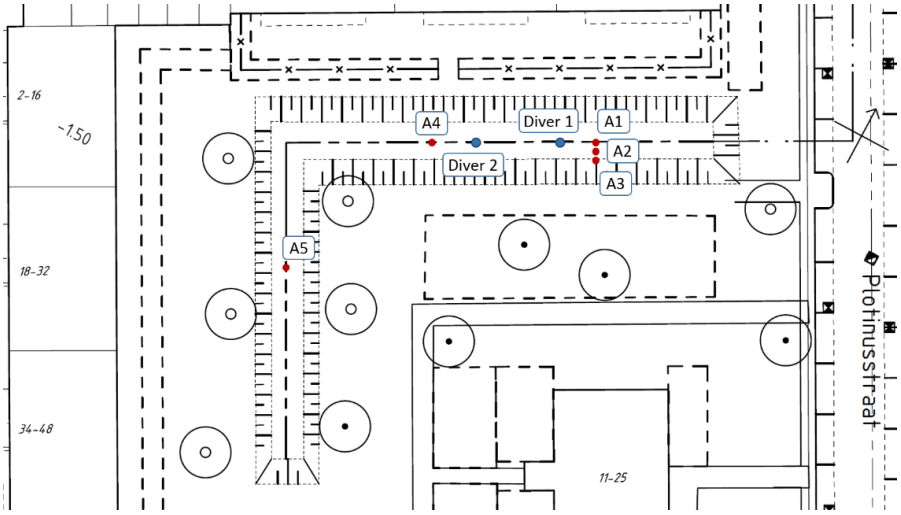

Figure 4.3: Diver and piezometer locations (Mobron, 2019)

4.3 Set-up of bioswale groundwater model

4.3.1 Model conceptualisation for case-study bioswale

The conceptualisation of the case-study bioswale in the model is shown in Figure 4.4, which includes three layers to represent the different soil types. These layers are referenced to the surface level as can be seen in Figure 4.4. Soil samples taken by Mobron (2019) indicate that the improved top layer and sand layer have a width of 2.2 meters, with the top layer having a depth of 0.3 meters and the sand layer 0.4 meters. Based on construction photos, the drain depth is estimated at -2.6 m NAP. The initial groundwater level was set at the drainage level of -2.4 m NAP, which corresponds to the initial groundwater levels observed in the piezometers before the storm simulations. A homogeneous clay layer (the native soil) around the improved layers was assumed for this study. Although the top layer of the native soil may differ due to mixing with sand, Mobron (2019) concluded that infiltration primarily occurs in the area of the improved top layer at the bottom of the bioswale.

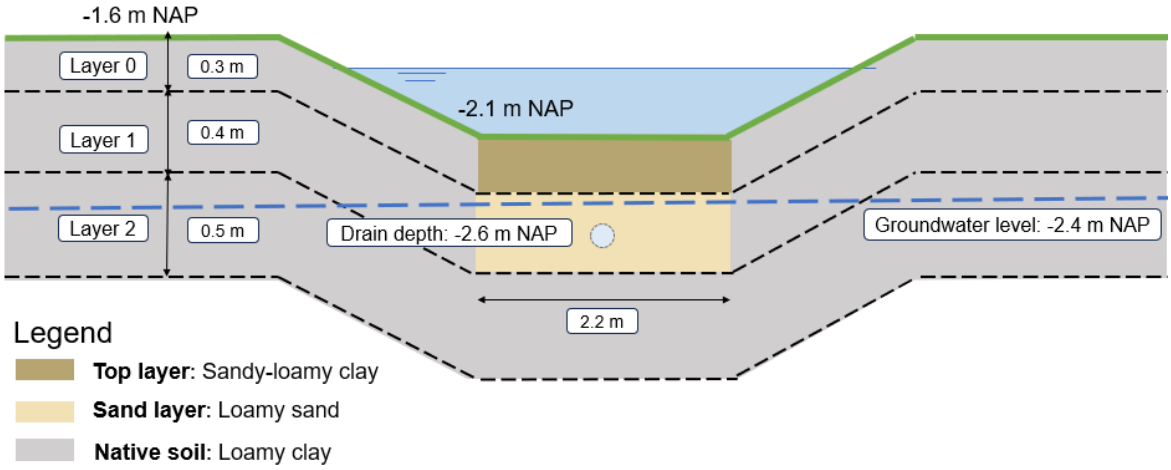

Figure 4.4: Conceptualisation of the case-study bioswale in the model

A surface grid with a resolution of 1x1 meter was used, derived from the Digital Terrain Model (DTM) provided by 'Actueel Hoogtebestand Nederland' (AHN). The latest DTM data was collected in 2020-

2022, after the construction of the case-study bioswale in 2017. The model outputs and layer discretization were calculated using this grid.

The model boundary was defined by the locations of the DIT-sewer pipes around the bioswale. Groundwater levels at the boundary were held constant at -2.4 m NAP, applying a constant head boundary condition (CHD) that allows water to flow through the boundary. At the bottom of the third layer, a no-flow boundary was specified.

4.3.2 Model parameters

A couple of soil parameters were not subject to calibration in this case study. The fixed values of these parameters are shown in Table 4.1.

Table 4.1: Fixed soil parameter values

Parameter	Description	Layer 0	Layer 1	Layer 2
$K_{s,\ native\ soil}$	Saturated hydraulic conductivity of the native soil (m/d)	0.02	0.02	0.02
S_y	Specific yield (-)	0.1	0.15	0.1
S_s	Specific storage (m^{-1})	10^{-5}	10^{-5}	10^{-5}
Θ_r	Residual moisture content (-)	0.045	0.051	0.068
Θs	Saturated moisture content (-)	0.384	0.374	0.380

The native soil was assumed to be isotropic, with a saturated hydraulic conductivity of 0.02 m/d, the same value used by Mobron (2019) when modelling this case-study bioswale. This value is consistent with the K-values defined by Smedema and Rycroft (1983), that range from 0.002 to 0.2 m/d for poorly structured loamy clay.

The specific yield (S_y) for the second layer was set slightly higher compared to the clayey layers at 0.15 due to the presence of the sand bed, which has higher porosity. Specific storage (S_s) was uniform across all layers and set at 10^{-5} m^{-1}.

Residual and saturated moisture content values (θ_r and θ_s) were based on soil texture samples taken by Mobron (2019). Using Rosetta Lite DLL (Schaap et al. 2001) in Hydrus 1D, Van Genuchten's water retention parameters were predicted based on soil texture and bulk density. These predictions resulted in the θ_r and θ_s values shown in Table 4.1.

The drainage level was set to a value of -2.4 m NAP, as this is the set drainage level in the area of the case-study bioswale. The infiltration factor was set to 0, meaning the drain only removes water and no infiltration occurs from the drain to the soil.

A time discretization of 10 minutes was chosen to simulate the hydraulic response of the bioswale during the simulated storms. This interval was sufficient to capture the inflow dynamics, which occurred over one hour or more. A 10-minute time step ensured numerical stability while keeping computation time reasonable.

4.3.3 Model calibration

The methodology described in section 3.2 was applied to the case-study bioswale to calibrate and validate the model. To ensure robustness and avoid overfitting, the storms were divided into calibration and validation sets, each containing different storm types. Storms 1 and 4 were chosen for calibration because they differ in peak flow and duration. This ensures the model is adaptable to various conditions. Storms 2 and 3 were used for validation to assess how well the calibrated parameters perform under different rainfall patterns, including the two-peak structure of storm 3.

At the start of this research, an attempt was made to model initial moisture contents that could represent the expected antecedent conditions for the four full-scale tests. However, it became evident that when an initial moisture content was specified (higher than the residual moisture content), the model redistributed the excess moisture to the groundwater, resulting in high initial groundwater levels. This behaviour can be attributed to inconsistencies between the soil parameter values and the specified initial moisture content. To address this, a warm-up period was introduced during model calibration. The bioswale was filled with water and emptied before the simulated rainfall (representing full-scale tests) began, making the soil wet. For storms 1, 3, and 4, rainfall started three days after filling to represent field capacity conditions, while for storm 2, rainfall began two days after filling to account for wetter antecedent soil moisture conditions during that full-scale test.

The model was calibrated and validated using drain discharge and surface water level measurements. Groundwater level measurements were excluded because the coarse 1x1 meter grid, in combination with an improved top layer of only 2.2 meters and a drain conceptualisation based on the coarse grid cells as well, resulted in a calculation of the groundwater levels that was not detailed enough. The modelled output could not be compared to the piezometer measurements that were spaced less than a meter apart.

5. Results and discussion

This chapter presents the results of the applied methodology on the case-study bioswale, along with a discussion on the interpretation and limitations of both the results and the methodology.

5.1 Calibration results

5.1.1 Model time-lag

A time-lag between the modelled and observed drain discharges was identified, with the model showing a greater delay in the unsaturated zone compared to the fast response in the measured drain discharge. Measurement errors could explain this time-lag; however, this is unlikely as the fast response time was observed in all four storm simulations conducted by Mobron (2019) and confirmed by measurements from Rujner et al. (2017). Alternatively, this time-lag is likely caused by the simplification of hydrological processes in the UZF package, where preferential flow paths are not included. Figure 5.1 shows the modelled drain discharge for storm 1, comparing a high saturated hydraulic conductivity of 15 m/d (simulating macropore flow) with the expected design value of 0.5 m/d based on soil texture. Both curves show a clear time-lag relative to observations. The higher hydraulic conductivity reduces the time-lag. However, when the design value based on soil texture is used, the time-lag increases, though the peak discharge more closely aligns with the observed maximum discharge. This supports the theory that macropore flow may be responsible for the quick drain response, followed by matrix flow dominance, which results in the lower peak. This dual process is not accurately captured by the homogeneous layers in the UZF package.

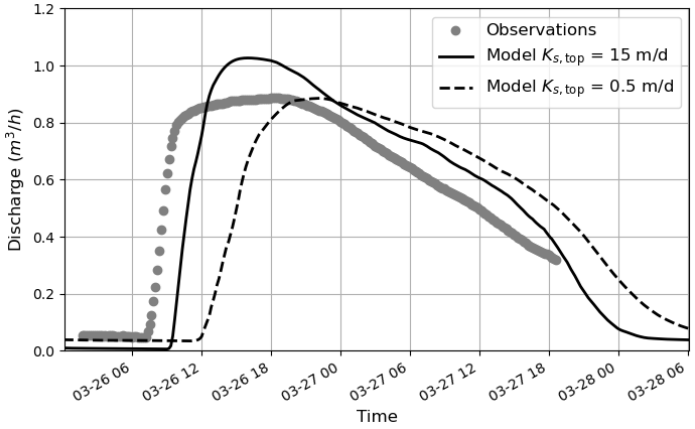

Figure 5.1: Modelled drain discharges for high and low hydraulic conductivity of the top layer (not shifted)

Because of this time-lag, the discharge curves were shifted to align with the start of measured drain discharge during calibration. In this way, the modelled discharge was purely calibrated on the shape of the curve. When defining the optimal parameter set, a threshold of two hours was defined as the acceptable maximum time-lag between the model results and the measured data. When this threshold for the time-lag was smaller, the values of the objective functions for these parameter combinations decreased.

5.1.2 Calibration parameter values

The results of the Monte Carlo calibration indicate that not all model runs were possible, as 7 out of 150 model runs failed to converge due to numerical instability. The optimal calibration parameters set, determined after optimizing the objective functions, is shown in Table 5.1 below.

Table 5.1: Optimal parameter values

Parameter	Description	Optimal Value
$K_{s,\,top}$	Saturated hydraulic conductivity top layer (m/d)	15
$K_{s,\,sand}$	Saturated hydraulic conductivity sand layer (m/d)	3.4
ε_{top}	Brooks Corey Epsilon top layer (EPS) (-)	4.2
ε_{sand}	Brooks Corey Epsilon sand layer (EPS) (-)	4
C_{drn}	Drain conductance factor (-)	0.18
I_{swale}	Infiltration parameter (m/d)	0.28
C_{bottom}	Bottom conductance (d)	4.2

As can be seen from Table 5.1, the calibrated values for saturated hydraulic conductivity for the top and sand layers differ from what soil texture measurements would suggest. For instance, the top layer's K_s value was calibrated to 15 m/d, while predictions based on soil texture class and design values range between 0.1 and 1 m/d. This can be explained by preferential flow paths present in the unsaturated zone. A similar pattern was observed in the model calibration of bioswales by Elçi & Molz (2009). They found an average factor of about 10 times higher for the model-calibrated K_s values compared to measured K_s values due to preferential flow processes. Since a time-lag constraint of less than two hours was set, a higher K_s value was obtained during calibration to account for these preferential flow processes.

The expected value for the hydraulic conductivity of the sand layer, $K_{s,sand}$, lays between 5 and 10 m/d (Mobron, 2019). A lower value of 3.4 m/d was obtained from calibration. As can be seen in Appendix A, many values of this parameter give equally good NRMSE values in this model conceptualisation. Some model results resulted in significantly higher NRMSE values. For the $K_{s,sand}$ parameter, no clear relationship between the parameter values and a better or worse NRMSE value can be found. This suggests a low sensitivity of this parameter.

5.1.3 Calibrated model outputs

Figure 5.2 shows the modelled water levels using the obtained calibration parameter values shown in Table 5.1. It also shows the water level measurements for the calibration data (storms 1 and 4). In Figure 5.3 results for the water levels for the validation data (storms 2 and 3) are shown. The corresponding values for the objective functions are presented in Table 5.2.

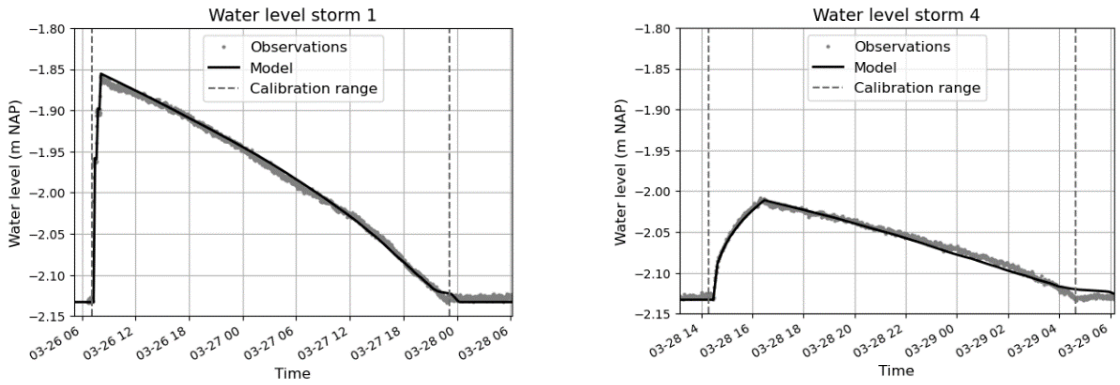

Figure 5.2: Modelled and measured water levels for calibration data

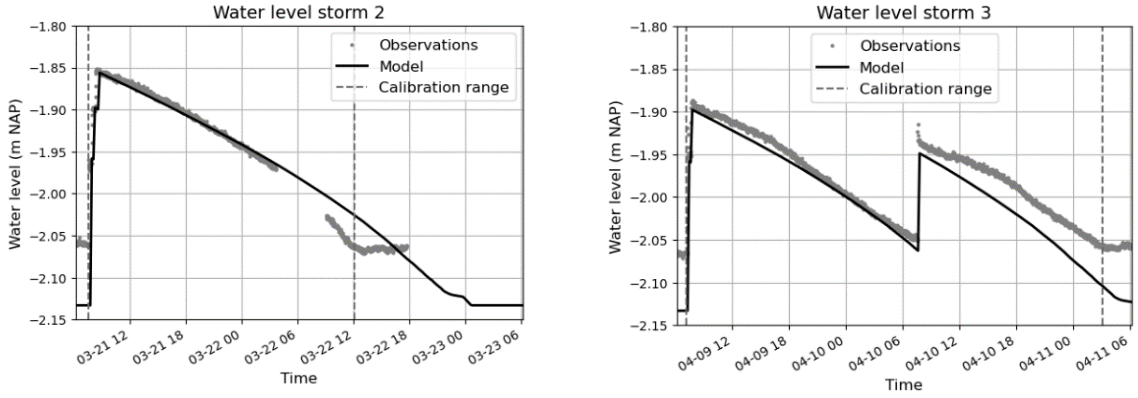

Figure 5.3 Modelled and measured water levels for validation data

Table 5.2: Objective function values water level

	Calibration		Validation	
	Storm 1	Storm 4	Storm 2	Storm 3
NSE (-)	0.970	0.976	0.807	0.681
NRMSE (-)	0.048	0.042	0.091	0.109
MAPE (%)	7.09	16.5	8.48	13.8

Table 5.2 shows that NSE values for calibrated storms suggest strong predictive performance, with values close to one, while validation storms showed lower NSE values, as expected. Storm 3, with an NSE of 0.681, still meets the acceptable threshold of 0.65 (Ritter & Muñoz-Carpena, 2013), though it is the lowest among all storms. This aligns with NRMSE values and may result from the diver's location, which was not at the bioswale's lowest point during measurements of storms 2 and 3 (Mobron, 2019). Storm 3, representing a two-storm event, showed consistent underestimation of water levels during the second peak. This may be due to wetter soil conditions at the diver location following the first storm peak, which would slow infiltration during the second storm. The model may not fully capture the effect of local soil moisture on infiltration rates. Unlike NSE and NRMSE, MAPE suggests weaker predictive performance for storm 4, likely due to the characteristics of the incoming storm 4 hydrograph.

The observed versus modelled drain discharges are shown in Figure 5.4 and Figure 5.5. With the same optimal parameter set, the objective functions are computed for the drain discharge for the calibration and validation storms, presented in Table 5.3. The corresponding time-lags between the modelled and measured discharge curves are presented in Table 5.3 as well.

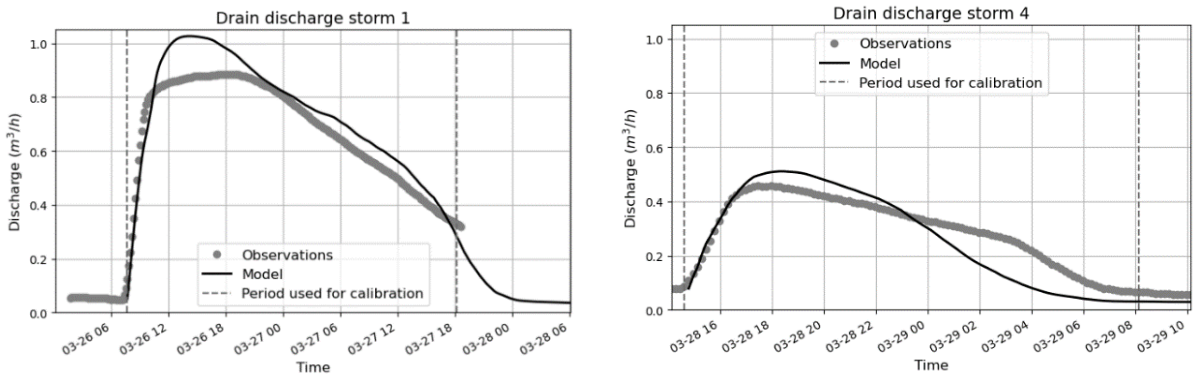

Figure 5.4: Modelled (shifted) and measured drain discharge for calibration data

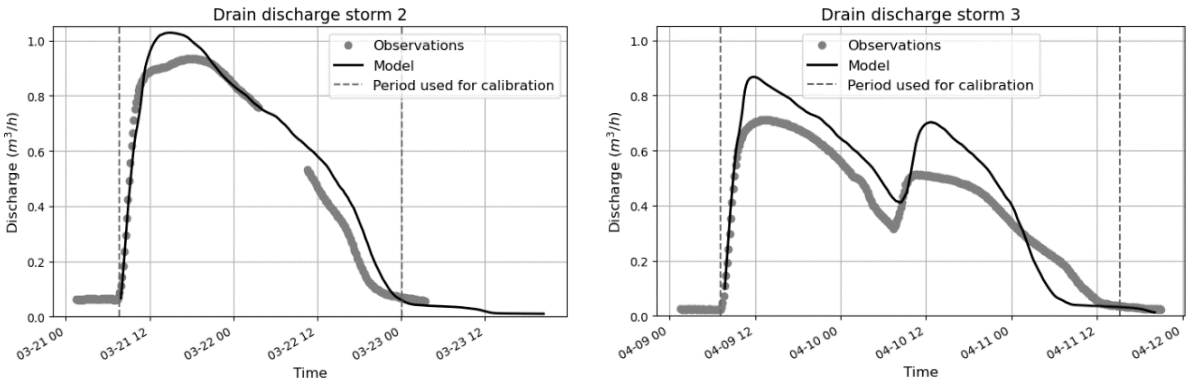

Figure 5.5: Modelled (shifted) and measured drain discharge for validation data

Table 5.3: Objective function and time-lag values

	Calibration		**Validation**	
	Storm 1	Storm 4	Storm 2	Storm 3
NSE (-)	0.847	0.564	0.934	0.726
NRMSE (-)	0.081	0.161	0.089	0.109
MAPE (%)	7.09	16.5	8.48	0.128
Time-lag (h:min)	1:50	1:50	1:30	1:50

The conceptualisation of homogenous layers in the UZF package and therefore simplification of preferential flow processes (as described in section 5.1.1) caused differences between the modelled and observed drain discharges. Firstly, Figures 5.4-5.5 show that all modelled drain discharges have a higher peak when compared to the corresponding measurements. This can be attributed to the high hydraulic conductivity obtained during calibration to account for preferential flow paths in the soil. The existence of a dual flow process in the unsaturated zone is supported by the measurements from storm 2, where the second discharge peak, resulting from matrix flow, is higher than the first peak, attributed to preferential flow.

Secondly, Table 5.3 shows that the time-lag in the model persisted even after calibration of the selected calibration parameters. An explanation for the modelled time-lag, even after calibration, may lie in the complexity of preferential flow processes combined with soil moisture content. For storms 1, 3 and 4 the time-lag remains nearly two hours, while for storm 2, it is slightly shorter at 1 hour and 30 minutes. This difference can be attributed to the fact that the storm 2 event was simulated two days after the initial filling of the bioswale, compared to three days for the other storms, to reflect wetter initial conditions.

5.1.4 Discussion of results

The calibration and validation dataset were limited both in terms of the number of measurements and test variety. Therefore, the calibration results cannot be generalized and it is not recommended to apply the calibrated parameters to other bioswales in Rotterdam. Parameter values may change over time due to temperature, vegetation and biological activity, but this variability was not captured as measurements were only taken from February to March 2019. Literature shows that infiltration rates vary among bioswales of the same type and over time (see section 2.1.3.), suggesting potential model overfitting. Furthermore, moisture content was not measured during the tests, so model output related to moisture content could not be validated.

The residual moisture content (θ_r) in the Brooks-Corey equation of the UZF package (see section 3.1.3.) was initially interpreted as the minimum moisture content. However, θ_r in the UZF package should reflect moisture content after gravitational drainage. Appendix C describes an uncertainty

analysis on the effects of changing this parameter with possible field capacity values. It is not advisable to include θ_r in the calibration, as the model might compensate for the time-lag by increasing the residual moisture content, resulting in unrealistic values. Measurements of the moisture in the soil would allow for more accurate determination of θ_r.

Moreover, the equifinality problem (Beven, 2006) presented further challenges. Multiple parameter combinations produced similarly good objective function values (see Appendix B), leading to uncertainty in parameter selection. This uncertainty could be reduced by incorporating additional types of data, such as groundwater levels and soil moisture, into the calibration process.

5.2 Sensitivity analysis results

5.2.1 Emptying time

Figure 5.6 shows the sensitivity of the simulated emptying time of a filled bioswale to the selected model parameters. The Tornado chart (see Figure 5.7) ranks the most sensitive parameters and displays their minimum and maximum ranges. An emptying time of 40 hours is obtained using the optimal calibrated parameter values from Table 5.1, indicated by the black vertical line in Figure 5.7.

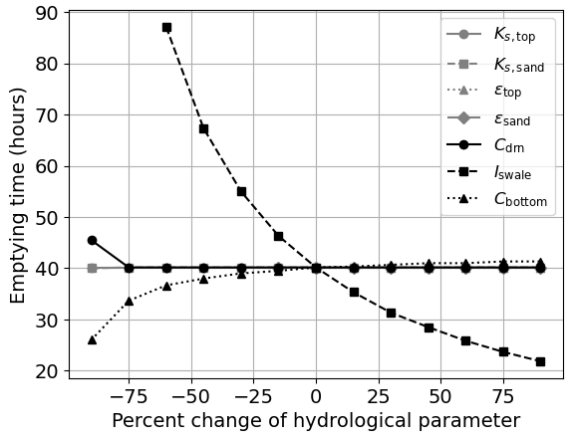

Figure 5.6: Sensitivity calibration parameters on emptying time

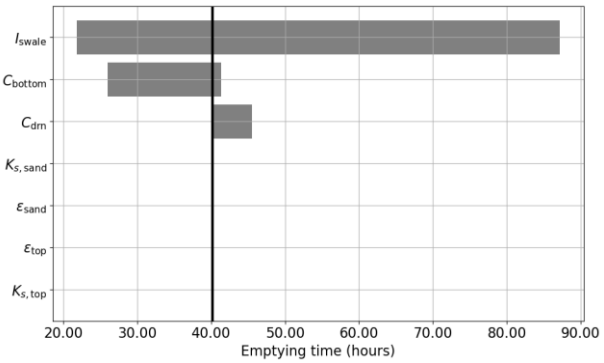

Figure 5.7: Tornado chart emptying time

Figure 5.6 and Figure 5.7 show that the emptying time is the most sensitive to the infiltration parameter (I_{swale}), which is expected as it determines the rate of infiltration described with the formula in section 3.1.2. The relationship is non-linear, as seen in the curve in Figure 5.6 and the asymmetric bar in the Tornado chart. This can be attributed to the shape and slope of the bioswale, where equal volume reductions result in a larger drop in surface water level when the surface water level is low, compared to when it is high.

The bottom conductance (C_{bottom}) mainly influences the emptying time when it was reduced, resulting in a non-linear relationship. As C_{bottom} decreases, the fraction $\frac{Waterlevel}{C_{bottom}}$ increases, raising the infiltration rate (see section 3.1.2). Conversely, when $C_{bottom}$is further increased, the fraction becomes so small that the infiltration rate is entirely controlled by the I_{swale} parameter.

Figure 5.6 and Figure 5.7 show that the total conductivity of the drain (C_{drn}) only affected the emptying time when it was decreased by 90%. This can be related to the fact that with too low conductivity the drain cannot drain the water away at the same rate it is infiltrating. Therefore, groundwater levels rise to the bioswale bottom, limiting the infiltration and increasing the emptying time.

The emptying time is not sensitive to the hydraulic conductivities and epsilon parameter of the two improved layers. Since I_{swale} is always lower than $K_{s,top}$, the latter is not a limiting factor and does not affect the infiltration and emptying time.

5.2.2 Peak discharge

Figure 5.8 shows the sensitivity of bioswale's peak outflow discharge to selected model parameters. The Tornado chart (see Figure 5.9) ranks the most sensitive parameters and displays their minimum and maximum ranges. A peak discharge of 1.02 m^3/h is obtained using the optimal calibrated parameter values from Table 5.1, indicated by the black vertical line in Figure 5.9.

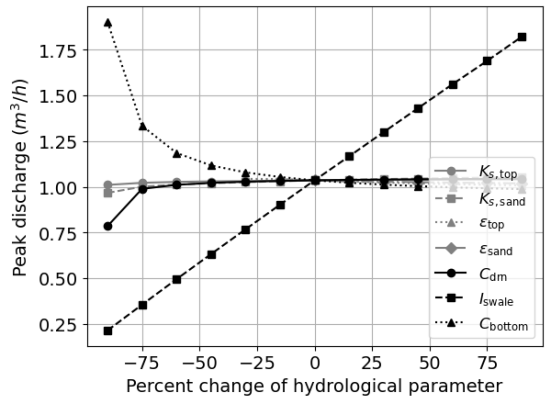

Figure 5.8: Sensitivity calibration parameters on peak discharge

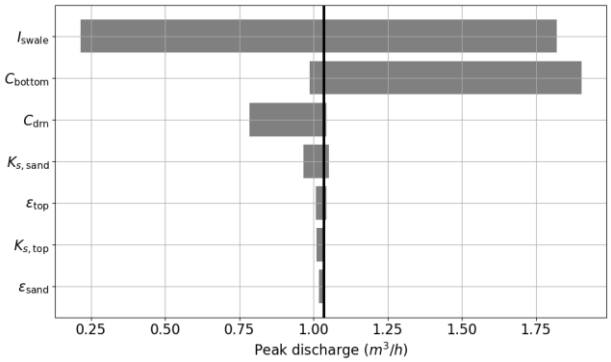

Figure 5.9: Tornado chart peak discharge

Figure 5.8 and Figure 5.9 show that the I_{swale} parameter has a linear relationship with peak discharge. The volume of water that infiltrates in the same time period changes linearlyby changing this parameter; hence resulting in a linear respons in peak discharge.

Figure 5.8 shows a non-linear relationship between C_{bottom} and peak discharge, due to its dependence on the surface water level in time, which decreases non-linearly because of the bioswale's shape. The parameter C_{drain} affects emptying time as described in section 5.2.1, and a lower infiltration rate results in a reduced peak discharge.

The soil parameters $K_{s,top}, K_{s,sand}$, ε_{sand} and ε_{top} slightly influence the peak discharge, by determining the unsaturated hydraulic conductivity, which impacts the timing and peak discharge in the drain.

5.2.3 Time-lag

The sensitivity of time-lag present in the modelled drain discharges to selected model parameters is shown in Figure 5.10 and Figure 5.11.

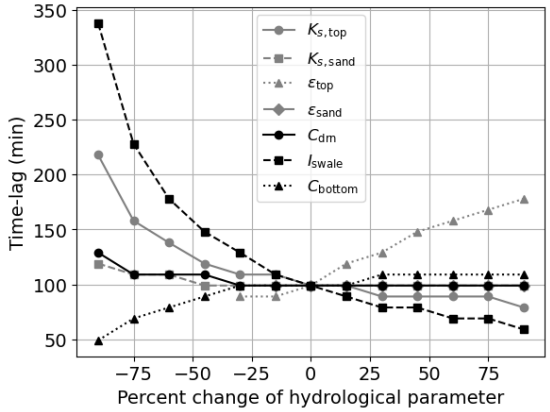

Figure 5.10: Sensitivity calibration parameters on time-lag in model

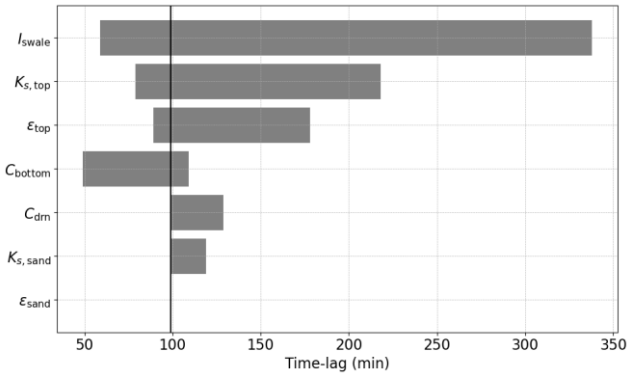

Figure 5.11: Tornado chart time-lag

Results from Figure 5.10 and Figure 5.11 suggest different sensitivity on the time-lag in the model for the different calibration parameters. A smaller hydraulic conductivity of the top layer ($K_{s,top}$) increases the time-lag in the model, however, increasing $K_{s,top}$ did not result in a similar decrease in the time-lag. This can be attributed to the change in moisture content with changing hydraulic conductivity which will be discussed below. The ε parameter influences the unsaturated hydraulic conductivity through the Brooks-Corey formula, thereby affecting the time-lag. Reducing the drain conductance (C_{drn}) resulted in a higher time-lag as a lower conductance increases the resistance of water entering the drain, leading to a higher time-lag.

The I_{swale} and C_{bottom} parameter influence the infiltration rate. The results in Figure 5.10 and Figure 5.11 indicate that these parameters also influence the time-lag in the model. This can be attributed to the change in water content in the unsaturated zone, by changing the infiltration rate and thereby affecting the time-lag. The change in water content in the unsaturated zone depends on the infiltration rate and hydraulic conductivity, as described by the following equations in the UZF package (Niswonger et al., 2006):

$$\theta = \frac{q_{in}}{K_s}^{1/\epsilon} \left(S_y\right) + \theta_r \qquad 0 < q_{in} \leq K_s$$

$$\theta = \theta_s \qquad K_s < q_{in}$$

where,

θ is the water content of an infiltration wave (-)

q_{in} is the infiltration rate (m/d)

Since the calibration parameters directly influence the time-lag observed in the model, as well as indirectly through changes in moisture content (from the formula above), the sensitivity of these parameters to the maximum moisture content in the top layer was also evaluated. Additionally, the effect of increased moisture content on the time-lag in the model was evaluated as well.

Moisture content in the unsaturated zone affects unsaturated hydraulic conductivity, as described by the Brooks-Corey formula, which in turn influences arrival time and the time-lag between the modelled and observed discharge curves. Figure 5.12 and Figure 5.13 illustrate the sensitivity of the calibration parameters to the maximum moisture content in the top layer during percolation.

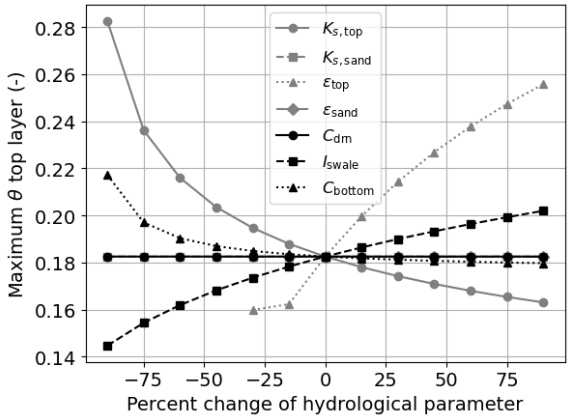

Figure 5.12: Sensitivity of calibration parameters on maximum moisture content in the topsoil layer during percolation

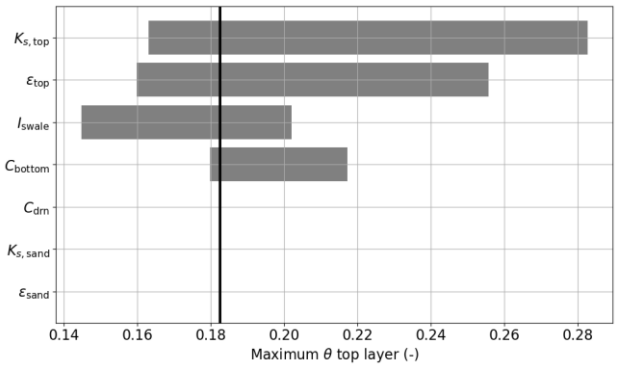

Figure 5.13: Tornado chart maximum moisture content top layer

As can be seen in Figure 5.12 and Figure 5.13, I_{swale} non-linearly influences the moisture content, reducing the time-lag at higher infiltration rates. Results from Figure 5.12 and Figure 5.13 also imply that hydraulic conductivity and the ε parameter are the most sensitive to maximum moisture content. Lowering the hydraulic conductivity and increasing ε lead to a higher moisture content but also lead to lower unsaturated hydraulic conductivity, influencing the time-lag both positively and negatively, unlike I_{swale}.
$K_{s,sand}$ and ε_{sand} showed no sensitivity to the maximum moisture content, since only the top layer's moisture content was evaluated.

To evaluate the effect of higher moisture contents on the time-lag in the model, a separate analysis was performed on the moisture contents. The value for residual moisture content was changed in order evaluate the influence of high moisture contents in the top layer of the soil. The results of this analysis are presented in Table 5.4. As expected, increasing the initial moisture content in the top layer reduced the time-lag. The model time-lag nears zero when the moisture content approached saturation, though saturation is unlikely under expected field capacity conditions.

Table 5.4: Effect of increasing moisture content on time-lag in the bioswale groundwater model

Residual moisture top layer content (-)	**Antecedent moisture content top layer (-)**	**Time- lag (min)**
0.045	0.08	110
0.10	0.13	90
0.15	0.17	70
0.20	0.22	60
0.25	0.26	40
0.30	0.31	20
0.35	0.35	0.32

5.2.4 Discussion of results

The sensitivity of the model parameters depends heavily on the conceptualization of the different layers of the bioswale, including the shape of the case-study bioswale. For example, when the slope of the embankment is different, the emptying time in Figure 5.6 will follow a different non-linear curve. Therefore, these results cannot be directly applied to other bioswales. Nonetheless, this methodology still highlights the most sensitive model parameters.

The I_{swale} parameter showed a high sensitivity regarding emptying time, peak discharge, time-lag in the model and maximum moisture content in the top layer. During the sensitivity analysis, the I_{swale} parameter was consistently lower compared to the saturated hydraulic conductivity of the top layer ($K_{s,top}$). When I_{swale} is increased and $K_{s,top}$ becomes the normative value, the infiltration (and consequently the emptying time and peak discharge) will be driven by $K_{s,top}$, reducing the sensitivity of I_{swale}.

A key limitation in the sensitivity methodology is the fixed-percentage parameter adjustment (OAT analysis). This impacted the results, as a small initial value yields less variation than a large one (Lenhart et al., 2002). For example, top and sand layer hydraulic conductivities had the same calibration ranges, but their sensitivity ranges differ due to initial values. Additionally, some parameters may affect the model output more significantly when larger ranges are applied, as seen in the broader calibration ranges for the bottom and drain conductance. An alternative approach, in which parameters are varied by a fixed percentage of the valid calibration parameter range, rather than the initial value, could improve the interpretation of sensitivities. Also, OAT analysis does not account for parameter interactions, unlike global sensitivity analyses (GSA), which evaluate parameter interactions across the full parameter space (Wang & Solomatine, 2019).

5.3 Bioswale performance assessment

5.3.1 Weather and climate analysis

This section presents the results for weather and climate scenarios defined in section 3.4.1. The parameter values in summer and winter are presented in Appendix G, including the results of the runoff area analysis.

Effect of initial groundwater level

Table 5.5 shows the results on bioswale performance when changing the initial groundwater level in winter and summer conditions. The design storms presented in Figure 3.5 and Figure 3.6 were used with a return period of two years in current climate.

Table 5.5: Results of changing initial groundwater level on bioswale performance

	Summer (T=2 years, 2014)			Winter (T=2 years, 2014)		
Groundwater level (m NAP)	**-2.7**	**-2.4**	**-2.0**	**-2.7**	**-2.4**	**-2.0**
Volume reduction (-)	0.63	0.89	0.91	0.63	0.84	0.87
Peak discharge (L/s/ha)	2.24	2.46	2.48	1.25	1.37	1.39
Maximum water level (m)	0.3	0.3	0.3	0.24	0.24	0.24
Emptying time (h)	26	26	26	27.33	27.33	27.33

As can be seen from Table 5.5, an increased volume reduction was obtained when lowering the initial groundwater level in both winter and summer conditions. As the drain is located at -2.6 m NAP, an initial groundwater level of -2.7 m NAP will cause the infiltrated water to recharge the groundwater until it reaches the set drainage level of -2.4 m NAP, and the drain starts to drain the water away. The volume of water that caused the groundwater level to rise above the set drainage level will not enter the drain, and therefore a higher volume reduction was obtained.

Furthermore, the results from Table 5.5 indicate that the peak discharge decreases with lowering groundwater table. The maximum water level in summer and winter conditions does not depend on the initial groundwater level as this is determined by the combination of the incoming hydrograph, runoff area and infiltration rate. The emptying time did not change with changing initial groundwater level as well.

Current and projected future climate

Figure 5.14 below shows the modelled response in terms of drain discharge and water level under the incoming hyetographs from Figure 3.5 and Figure 3.6. All four scenarios are computed with the same runoff area presented in Appendix G.

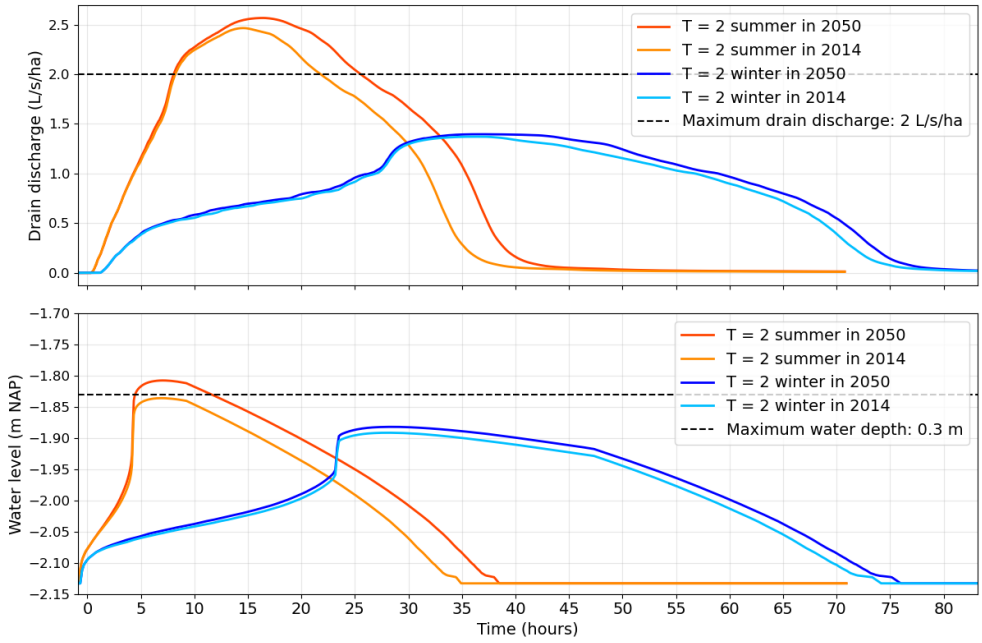

Figure 5.14: Modelled water level and drain discharge in current and future summer and winter conditions

Table 5.6 shows the results of the performance of the case-study bioswale in terms of volume reduction, peak discharge, maximum water level and emptying time in current and future climate in summer and winter conditions.

Table 5.6: Results of summer and winter performance in current and future projected climate

	Summer		Winter	
	T=2 years, 2014	**T=2 years, 2050**	**T=2 years, 2014**	**T=2 years, 2050**
Volume reduction (-)	0.89	0.88	0.84	0.84
Peak discharge (L/s/ha)	2.46	2.57	1.37	1.39
Maximum water depth (m)	0.3	0.32	0.24	0.25
Emptying time (h)	26	29.5	27.3	29

The results from Figure 5.14 and Table 5.6 indicate various aspects regarding the performance of the case-study bioswale. Firstly, the volume reductions hardly changed between the current and future climate scenarios. Regarding the peak discharge, the bioswale did not meet the criteria for peak discharge in both the current and future expected peak rainfall under summer conditions. In winter conditions in both the current and expected future climate, the peak discharge met the criterion of 2 L/s/ha. Although the volumes between summer and winter design storms are comparable, the longer duration of the winter events, the lower incoming peak, and the lower infiltration rate resulted in a lower peak discharge.

Only in the climate scenario for 2050 under summer conditions did the surface water level exceed the maximum depth of 0.3 meters. This is as expected since the runoff area was determined based on a full bioswale when a design storm of T=2 from 2014 was used. The maximum water level in the 2050 scenario was 2 centimetres higher than allowed, and if an overspill were to be

incorporated, this would result in a volume of water of 7.5 m³ that would directly enter the drainage network for almost 7 hours.

The emptying time increased as the volume of the design storms rises in the 2050 design storms under both summer and winter conditions. However, the maximum emptying time of 36 hours was never exceeded.

Rainfall over 4 months

Figure 5.15, shown below, shows the modelled bioswale response during winter conditions in terms of drain discharge and water level in time under measured rainfall between November 2023 and February 2024. The performance of the case-study bioswale can be tested on the ponding duration criterion as well.

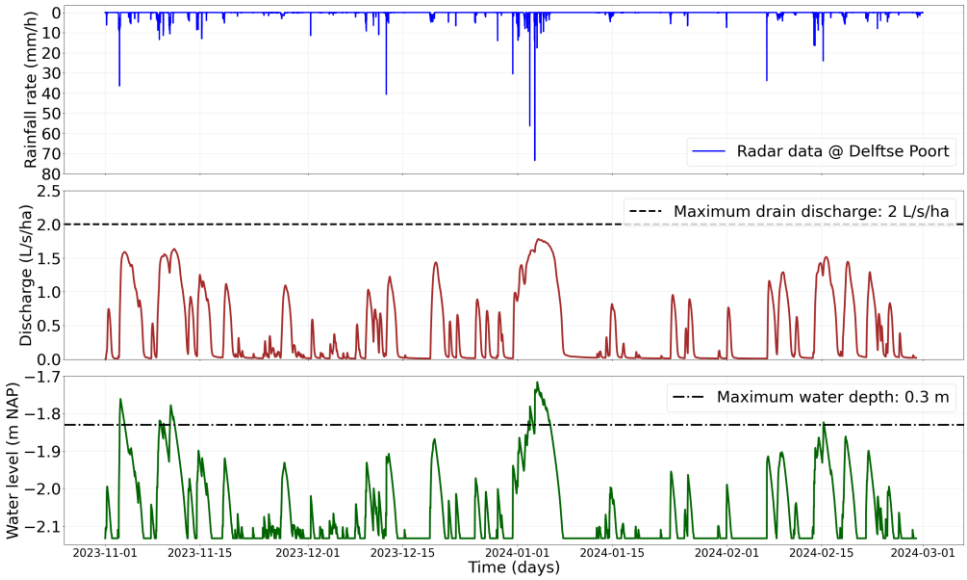

Figure 5.15: Modelled water level and drain discharge from November 2023 – February 2024

The results from Figure 5.15 indicate, firstly, that the outflow drain discharge never exceeded the maximum allowable discharge of 2 L/s/ha, despite high rainfall rates. This can be attributed to the lower (calibrated) value used for the I_{swale} parameter, causing lower infiltration rates and lower peak discharges (see the results of the model parameter sensitivity analysis in section 5.2.2).

As can be seen in the third plot (the surface water level vs. time) the water level exceeded the maximum depth of 0.3 meters three times, with a total of118 hours (4.1% of the period). The longest duration of overflow was from January 3rd to 5th, 2024, coinciding with the highest peak rainfall (>70 mm/hr, Figure 5.16). Ponding in the swale lasted up to 7.5 days from December 31st, 2023, to January 7th, 2024, exceeding the 7-day maximum allowable duration, though mosquito formation is unlikely in winter. The emptying time criterion was not assessed as the definition of the emptying time from section 2.1.2. could not be applied to rainfall data with multiple events.

When considering the entire analysed time period, water was ponding in the swale for a longer duration than the rainfall events themselves. While it rained for 18.6% of the hours, water ponded for 55% of the time, indicating that the bioswale continues to function effectively as a storage system in winter by flattening rainfall peaks. However, as no paved surface is connected to the bioswale, the model results may differ from what would be observed in reality if measured over the same period.

5.3.2 Design scenario analysis

This section presents the results for the two design scenarios defined in section 3.4.2.

Design scenario A: Modified drain location and sand type (with original bioswale width)
Figure 5.16 shows the bioswale cross-section model conceptualisation when the drain was moved two meters horizontally. The sand layer was also widened compared to the original cross-section shown in Figure 4.4.

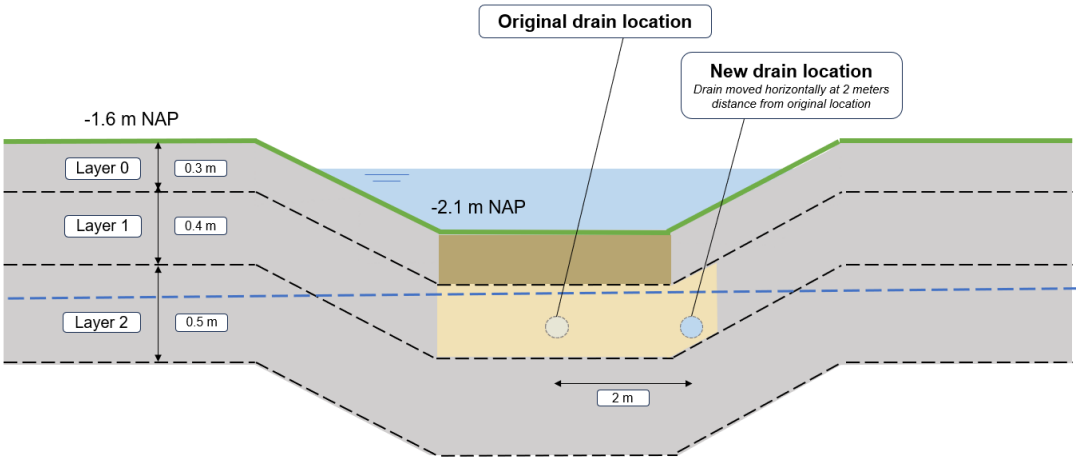

Figure 5.16: Bioswale cross-section model concept design scenario A

The effects of moving the drain further away horizontally in the case-study bioswale, in terms of peak discharge and emptying time, are shown in Figure 5.17 and Figure 5.18, respectively.

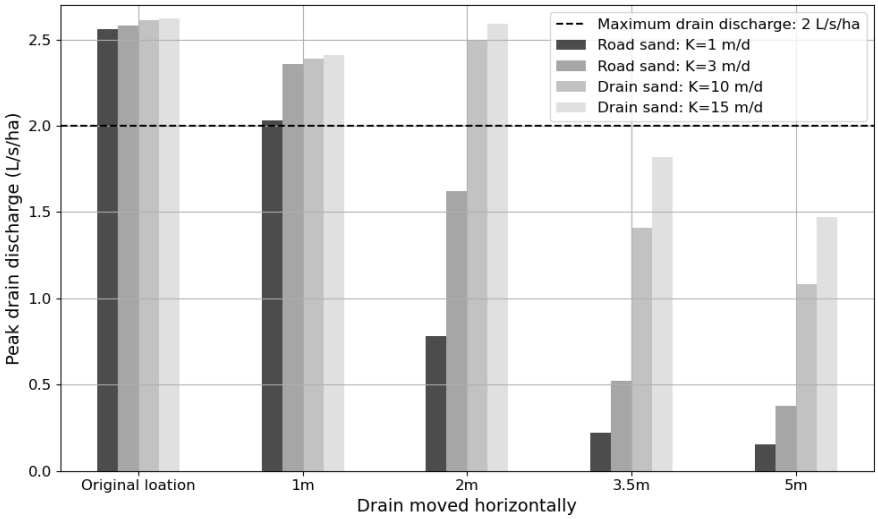

Figure 5.17: Peak discharges for different drain distances in combination with sand type

The results in Figure 5.17 show a clear decrease in peak discharge as the horizontal distance of the drain from the middle (and deepest point) of the bioswale increases. This effect is most pronounced when road sand was used. In terms of costs, both types of sand have a similar price, so neither option offers a significant cost advantage. With a drain distance of 3.5 meters from the middle of the swale, the peak drain discharge met the criterion of a maximum discharge of 2 L/s/ha, regardless of the sand type chosen. However, as the drain is placed further away, more sand is required. Therefore, to select the most cost-effective option that still meets the criterion, it is recommended to position the drain close to the middle, while meeting the maximum peak discharge criterion.

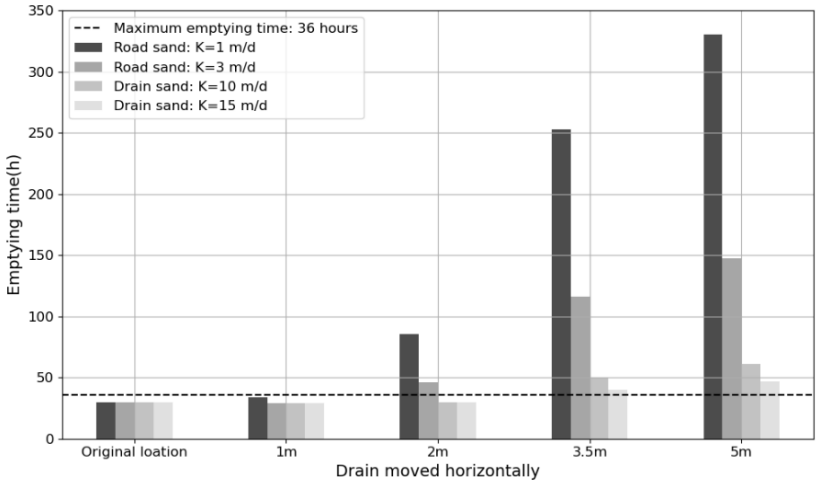

Figure 5.18: Emptying times for different drain distances in combination with sand type

When considering emptying times (shown in Figure 5.18), however, the emptying time increased as the drain distance increased, with values exceeding 8 days when road sand was used. The maximum emptying time of 36 hours was only met with a drain positioned in the middle (the original location) or at a distance of one meter.

The increased distance the water must travel as the drain distance increased resulted in a longer travel time. This causes groundwater levels in the middle of the bioswale to rise, limiting infiltration into the bioswale and leading to longer emptying times, which in turn result in lower peak discharges. This is illustrated in Figure 5.19 below and shows an increase of the groundwater level until the bottom of the bioswale (at around -2.1 m NAP), limiting the infiltration. For further drain distances and lower K values, it takes longer for the water to reach the drain, which delayed the lowering of groundwater levels, further limiting infiltration and increasing the emptying time.

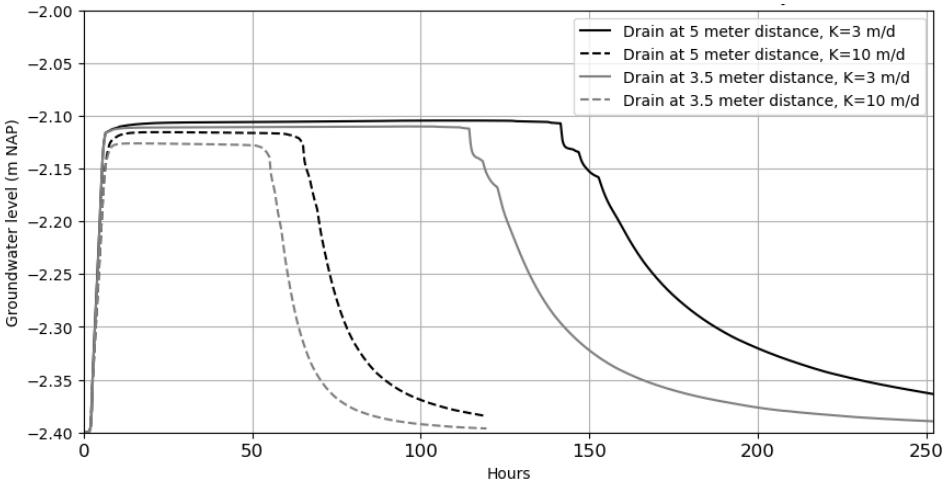

Figure 5.19: Groundwater level rise in the middle of the sand layer for different drain distances and K values

Figure 5.17 and Figure 5.18 show that a balance must be found between emptying time and peak discharge. A design using road sand with a drain positioned one meter from the middle is the only design that satisfies the emptying time criterion and results in a lower peak discharge compared to the original design. However, when the case-study bioswale with a drain moved with one meter was tested under the wet winter data from November 2023 to February 2024, the modelled water levels show that the maximum ponding duration of 7 days was further exceeded. This makes it difficult to select an optimal drain location where both the emptying time, maximum discharge and maximum ponding duration criteria are met.

Design scenario B: Increased bottom bioswale width

Figure 5.20 shows the bioswale cross-section model conceptualisation when the bottom of the bioswale was widened and two drains were used. The storage in the wider bioswale increased, therefore an extra paved surface area of 1480 m^2 could be connected to the bioswale.

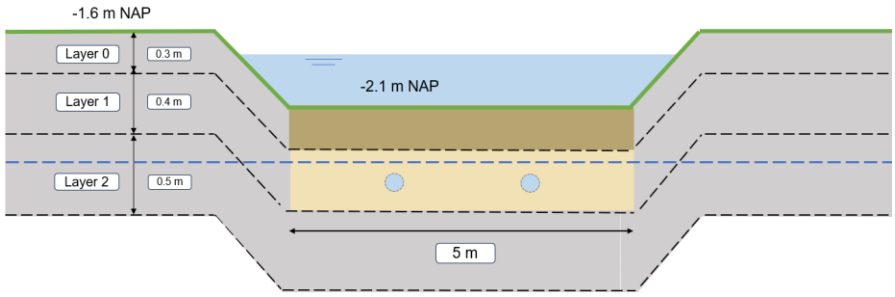

Figure 5.20: Bioswale cross-section model concept design scenario B

The resulted emptying time and peak discharge with different distances between drains when a wider bioswale was designed are showed in the Figure 5.21 and Figure 5.22 below.

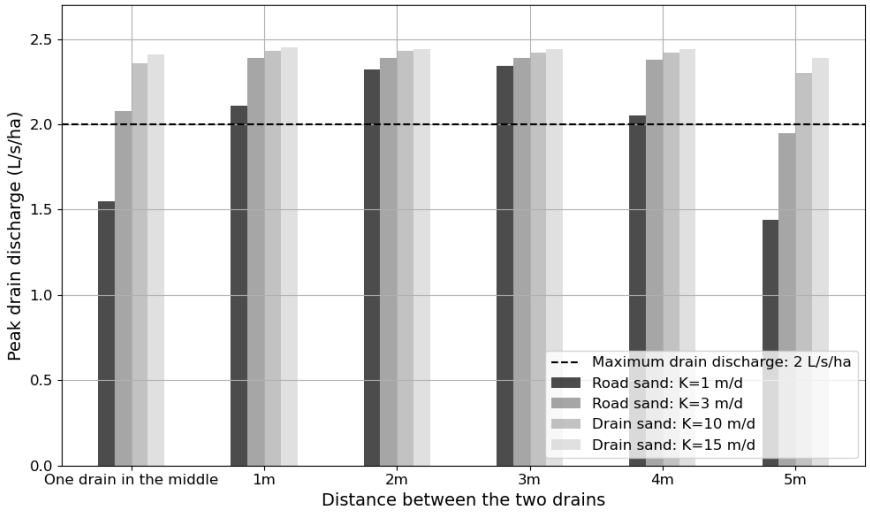

Figure 5.21 Peak drain discharges for increasing distance between two drains

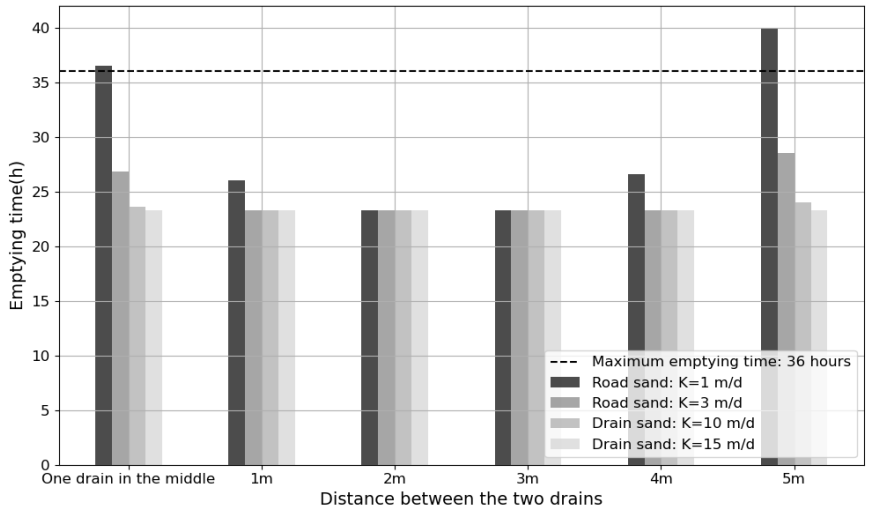

Figure 5.22 Emptying times for increasing distances between two drains

Figure 5.22 shows that, even with a single drain, the bioswale with a width of 5 meters emptied within 36 hours for both road sand and drainage sand. This differs from expectations, as the Municipality of Rotterdam recommends using two drains for bioswales wider than 3 meters, to facilitate infiltration. This can be explained by two factors:

1. The total volume of the case-study bioswale increased as the bottom became wider (from 33 m^3 to 53 m^3). Therefore, a larger paved surface area was connected to the bioswale to maintain its capacity under the T=2 2014 summer design storm. However, compared to the original design, the infiltration surface of the newly designed case-study bioswale increased more than the volume of water in the bioswale (width of 5 meters compared to 2.2 meters).

2. With the widened, improved top layer in the new design, storage in this layer increased. When groundwater levels rise into the top layer, water can easily flow horizontally toward the drain. As a result, the groundwater level does not reach the bottom of the bioswale, and infiltration is not limited as was modelled when the drain was moved in the original design (see Figure 5.19).

Regarding peak drain discharge for one drain in the centre of the wider bioswale, the maximum value is exceeded for K values of 3, 10, and 15 m/d. When two drains are used, the emptying time decreases, and the peak discharge increases, but there is no further change with increasing drain distance until the drains are 5 meters apart.

5.3.3 Discussion of results

Since only one bioswale was modelled, the findings of the performance assessment cannot be generalized to other bioswales. Furthermore, the time-lag observed during calibration is likely present in the modelled scenarios. However, as the response under these design storms and rainfall events was not measured, the exact time-lag remains unknown. Even though the precise time-lag is uncertain, different scenarios can still be compared.

It is notable that the bioswale did not exceed the maximum water depth criterion during the winter design storm but did exceed 0.3 meters when tested with winter rainfall data. This can be attributed to several factors. When looking at the rainfall data a maximum rainfall rate higher than 70 mm/hr was observed in the first days of January 2024. This peak is higher than the peak discharge of the winter design storms (Figure 3.6) for a two-year return period and is more consistent with the summer design storm peaks. However, the return period of such an event in winter is unknown.

The model likely overestimates peak drain discharges, as calibration indicated. Additionally, it is possible that a higher maximum drain discharge than 2 L/s/ha could be acceptable. Due to pipe friction in the drainage and sewer system, it is expected that a higher peak discharge at the bioswale could still meet the 2 L/s/ha limit upon reaching surface water. Additionally, there is uncertainty in the runoff coefficient. Using a lower coefficient allows a larger runoff area to be connected to the bioswale while maintaining the same water volume, leading to a lower peak discharge in terms of discharge per runoff area.

The design scenario analyses showed that the location of the drain is a critical factor regarding the performance of the bioswale. However, with increasing drain distance the value for horizontal hydraulic conductivity (K_h) becomes more important and could have significantly impacted the results. The horizontal conductivity of the top layer is expected to be different compared to the vertical direction because of macropore development. For example, Germer & Braun (2015) showed that this anisotropy can cause K_h to be two times as small compared to K_v in macroporous soil.

6. Conclusion and recommendations

The objective of this study was to evaluate the performance of bioswales in Rotterdam using a hydrological groundwater model that includes simulation of the unsaturated zone flow processes. Based on the results, the main research question is answered, followed by recommendations for future research.

6.1 Conclusions

The following answers to the research questions and conclusions were drawn on the basis of literature and results obtained from the bioswale groundwater model. The main research question was formulated as follows:

How do bioswales perform under various conditions, as evaluated by a hydrological groundwater model?

Firstly, it can be concluded that the bioswale groundwater model developed by Deltares can be used to assess the hydrological performance of bioswales. Furthermore, the increased knowledge about bioswale performance will guide better decision-making, particularly in bioswale design and implementation. This, in turn, will help refine the city's climate adaptation strategies.

The main research conclusion was drawn based on the conclusions of the predefined sub-questions.

1. *How accurately does the groundwater model simulate the hydrological response of a bioswale?*

It is concluded, based on the case-study analysis, that the bioswale groundwater model can describe water levels and discharges in bioswales rather realistically. Consequently, the model can be used to assess the performance of the studied bioswale under new conditions. However, the calibration revealed that preferential flow processes significantly affect bioswale performance, though these processes are not incorporated into the Unsaturated Zone Flow (UZF) package used in the bioswale groundwater model. Due to this simplification of homogeneous layers, the modelled drain discharges showed a time-lag compared to the measured discharges. By using a higher hydraulic conductivity to account for the missing preferential flow processes, this time-lag could be reduced to around two hours. However, this higher hydraulic conductivity leads to lower moisture content in the unsaturated zone, which may not reflect real-life conditions.

2. *What are critical factors influencing the performance of bioswales?*

The case-study results show that the performance of bioswales in terms of both emptying time and peak discharge depends heavily on the specific infiltration rate. This is largely influenced by parameter I_{swale} and partially by C_{bottom}. Higher moisture contents decreased the arrival time of water flow in the unsaturated zone. However, the moisture content values could not be validated as no measurement data was available, limiting the ability to fully assess its accuracy under different initial moisture conditions.

3. How do bioswales perform under different representative weather and climate conditions?

The performance of the current design of the case-study bioswale was assessed by modelling its response to design storms for both current and projected future climates (2050), under summer and winter conditions with a two-year return period. In future climates, summer rainfall is expected to have higher peak rainfall intensities, reflecting more extreme, short-duration rainfall events. In contrast, winter events are characterized by lower peak intensities but longer durations, with an overall increase in rainfall, making winters generally wetter. Using the summer and winter design storms, the bioswale's performance for individual events was evaluated based on three criteria: a maximum emptying time of 36 hours, a peak discharge limit of 2 L/s/ha, and a maximum water depth of 0.3 meters.

From the results, it can be concluded that during summer conditions, both current and future projected climate scenarios exceeded the peak discharge performance criterion, with values reaching 2.46 and 2.57 L/s/ha, respectively. Additionally, the maximum water depth was exceeded for almost seven hours in the future summer scenario. However, the emptying time criterion of 36 hours was never exceeded during summer conditions. In winter conditions, the bioswale met the criteria for peak discharge, emptying time, and maximum water depth when using design storms. When the hydrological response of the case-study bioswale was simulated under a significantly wet winter period (November 2023 to February 2024, using radar rainfall data), the water level exceeded the criterion of 0.3 meters, though the peak discharge limit was never exceeded. From these results it can be concluded that simulating consecutive rainfall events can be more critical when testing performance under winter conditions, compared to using a single design storm.

4. Can the existing bioswale design be improved to better meet performance requirements?

The case-study results showed that increasing the distance of the drain from the centre of the bioswale can significantly reduce peak discharge, especially when road sand is used. However, this comes at the cost of increased groundwater levels, which can extend the emptying time beyond the acceptable limit of 36 hours, depending on design choices such as drain placement, bioswale width, and sand type. Therefore, a balance must be found between emptying time and peak discharge, as no design was found to meet both criteria perfectly. Nonetheless, the results highlight the significant impact of drain location on bioswale performance. Widening the bioswale bottom to five meters allowed for a larger volume to accommodate more impervious surface area. The redesigned bioswale already met the emptying time criterion of 36 hours, and adding additional drains did not result in significantly improved performance.

In conclusion, preferential flow due to macropores in the unsaturated zone plays a crucial role in bioswale performance, and simplifying the zone as a homogenous layer overlooks these critical dynamics. While the current bioswale design is effective for individual winter events, it struggles to meet performance criteria during intense summer rainfall events. Adjustments to drain placement, bioswale dimensions, and sand type can optimize peak discharge, but care must be taken to manage the trade-off with increasing emptying time. Although this study focused on one case-study bioswale, the findings are likely applicable to other bioswales with similar design and environmental conditions. However, site-specific factors may lead to variations in performance, and further research is needed to generalize these results across a wider range of bioswales.

6.2 Recommendations

Based on the obtained results and conclusions, the following recommendations for further research as well as for future municipal practice are presented below.

6.2.1 Further research

This study hardly included calibration based on groundwater levels. To accurately simulate water flow in the saturated zone that reaches the bioswale's drain, groundwater levels should be modelled on a larger scale in the area surrounding the bioswale. Continuous measurements of rainfall events are needed instead of full-scale tests, which would allow for comparing measured groundwater levels with modelled results. For this purpose, it is recommended to allow for heterogeneity in soil parameters in the horizontal direction, and not only between vertical soil layers. Moreover, it is recommended to adjust the values for the vertical and horizontal hydraulic conductivity of the top layer, as they may vary due to expected anisotropy from preferential flow paths.

Furthermore, a more detailed measurement study on the temporal and spatial variation of infiltration rates due to vegetation and seasonal changes is recommended. This study could also include specific research on comparison of different vegetation types. Current literature does not specifically address these factors in the Netherlands, and studies conducted in Rotterdam may yield different results, compared to studies conducted in other countries. It is important to test infiltration at different locations within the bioswales, as the formation of macropores and variations in vegetation density can affect results. Ahmed et al. (2015) showed that at least 20 measurements are needed to obtain a representative mean value. Additionally, it is recommended that these tests are conducted during different seasons to account for variations in temperature, vegetation, and biological activity. This study could also include a detailed study on the formation and influence of macropores over time.

When modelling bioswales, the simplification of homogeneous layers in the UZF package can be improved to better account for preferential flow in the unsaturated zone. A relatively simple approach could be to bypass a portion of infiltrated water directly to the groundwater table when soil moisture exceeds a specific threshold, simulating the rapid flow through macropores. Alternatively, a dual-permeability or dual-porosity model could be developed to differentiate between the interacting flow processes through macropores and the soil matrix. In dual-porosity models, it is assumed that water in the matrix is stagnant. In dual-permeability models, on the other hand, water flow in the matrix is modelled as well. This can, for example, be modelled using HYDRUS 2D/3D.

6.2.2 Practical recommendations

Bioswale design

From literature (see section 2.1.3) and measurements in Rotterdam (see Appendix E), it became evident that infiltration rates vary significantly both spatially and temporally. This variability makes it difficult to directly link specific design criteria, such as soil composition and vegetation type, to infiltration rates and peak discharges. However, as this research demonstrated, the location of the drain has a significant impact on bioswale performance. Unlike soil and vegetation, which are subject to natural variability, the placement of the drain is a design element over which a designer has much greater control. Therefore, it is recommended to ensure that the soil in the bioswale is highly permeable and planted with vegetation that positively influences permeability and the formation of macropores. Based on the specific situation, the number and location of drains can then be optimized to achieve the desired performance. The current bioswale groundwater model can be a valuable tool to support this optimization process.

Measurement data

During this research, it became clear that not enough information was available to capture the variability of bioswales performance. Therefore, more empirical research is recommended as this would improve the interpretation of model results. Firstly, more continuous long-term measurements are required throughout different seasons, particularly of bioswales that contribute significantly to the urban water system through their connected paved surfaces. Emphasis should

be placed on studying bioswales with varying designs, such as those where the drain is positioned at the side of the bioswale, to validate these model results. By measuring over an extended period, the bioswale's functionality over their lifetime could be assessed and model results could be validated with more diverse data. Secondly, when assessing performance during wet and dry conditions, it is crucial to include soil moisture measurements in the measurement campaigns, apart from water level, discharge and groundwater level measurements. This provides an additional validation source for checking modelled output.

Application of the bioswale groundwater model
Despite the simplifications of the unsaturated zone in the UZF package, the bioswale groundwater model can still be applied in various cases. For example, the approximate impact of design changes can be analysed. During the design of new bioswales, the effects of a wider bioswale, additional connected paved surface, a deeper drain, or a broader sand layer can be evaluated. Furthermore, the performance under different (design) rainfall events can be easily assessed. However, detailed modelling of the unsaturated zone in bioswales using the UZF package will remain challenging. When applying the bioswale groundwater model in its current form, it is recommended to use the lower, expected hydraulic conductivity of the top layer. This will result in a time-lag, but the peak discharge and moisture content in the unsaturated zone can be modelled more realistically. A simple way to incorporate preferential flow into the model would be to bypass a percentage of the infiltrating water directly to the groundwater table.

It can be argued that applying the current bioswale groundwater model to other types of SuDS, such as the Aquaflow system or permeable pavement may be even more suitable than modelling bioswales. In the Aquaflow system, water enters the system through gully pots at the street and flows in the road foundation layer, before infiltrating in the high permeable granulate layer. With permeable pavement, water enters the permeable soil layers through porous urban surfaces designed to allow water to pass through.

Since these systems do not have a vegetation layer and are closed off by the road surface, their performance is likely less determined by macropores. Therefore, the soil in the unsaturated zone is likely to be more homogeneous and less variable spatially and temporally, making the UZF package more applicable. However, this should be validated with measurements. The current bioswale groundwater model requires only minor adjustments to be applicable to other SuDS types, primarily in how water enters the system. For example, in Aquaflow systems, water enters through gully pots rather than ponding on the surface, as simulated in the current bioswale groundwater model. The structure of the layers in the unsaturated zone, however, can be applied in their current form to other SuDS types. When modelling other SuDS types, it is recommended to include soil moisture measurements, in addition to discharge and groundwater levels, to validate the modelled results.

Modelling urban scale
In the context of improving Rotterdam's climate resilience, it could be valuable to study detailed modelling of individual bioswales in combination with urban-scale modelling of the city's water system. In practice, the entire urban water system plays a key role in mitigating urban pluvial flooding. Factors such as the amount of paved versus vegetated area, drainage to surface water, and the types, locations, and dimensions of SuDS, all influence areas prone to flooding. As the peak reduction and delay by individual SuDS contribute to the overall performance of the water system, it is advisable to analyse their individual contribution to the entire system. This can be analysed using models like Infoworks ICM, which is already in use by the Municipality of Rotterdam. Parameter values that describe the performance of bioswales (and other SuDS types) can be derived from the calibrated and validated detailed bioswale groundwater model used in this study. When combined with additional measurement data for model validation, integrating these two types of models could significantly strengthen Rotterdam's climate resilience on an urban scale.

Furthermore, when including SuDS modelling in Infoworks ICM, energy loss and peak flow reduction through the pipe network to surface waters can also be calculated and integrated into the analysis. This allows for a more precise and detailed determination of the maximum peak discharge criterion. As the flow moves through the pipe network, depending on its length and characteristics, the peak discharge is reduced due to energy losses, eventually reaching the maximum of 2 L/s/ha upon entering surface waters. This approach will improve the interpretation and application of the maximum allowed peak discharge imposed by the waterboard.

References

Ahmed, F., Gulliver, J. S., & Nieber, J. (2015). Field infiltration measurements in grassed roadside drainage ditches: Spatial and temporal variability. *Journal of Hydrology*, *530*, 604–611. https://doi.org/10.1016/j.jhydrol.2015.10.012

Assi, A. T., Blake, J., Mohtar, R. H., & Braudeau, E. (2019). Soil aggregates structure-based approach for quantifying the field capacity, permanent wilting point and available water capacity. *Irrigation Science*, *37*(4), 511–522. https://doi.org/10.1007/s00271-019-00630-w

Beersma, J., Hakvoort, H., Jilderda, R., Overeem, A., & Versteeg, R. (2019). *Neerslagstatistiek en-reeksen voor het waterbeheer 2019*. https://www.stowa.nl/sites/default/files/assets/PUBLICATIES/Publicaties%202019/STOWA%202019-19%20neerslagstatistieken.pdf

Beven, K. (2006). A manifesto for the equifinality thesis. *Journal of Hydrology*, *320*(1), 18–36. https://doi.org/10.1016/j.jhydrol.2005.07.007

Bockhorn, B., Klint, K. E. S., Locatelli, L., Park, Y.-J., Binning, P. J., Sudicky, E., & Bergen Jensen, M. (2017). Factors affecting the hydraulic performance of infiltration based SUDS in clay. *Urban Water Journal*, *14*(2), 125–133. https://doi.org/10.1080/1573062X.2015.1076860

Boogaard, F. C. (2015). *Stormwater characteristics and new testing methods for certain sustainable urban drainage systems in The Netherlands* [Doctoral thesis, University of Technology Delft]. https://resolver.tudelft.nl/uuid:d4cd80a8-41e2-49a5-8f41-f1efc1a0ef5d

Boogaard, F. C. (2022). Spatial and Time Variable Long Term Infiltration Rates of Green Infrastructure under Extreme Climate Conditions, Drought and Highly Intensive Rainfall. *Water*, *14*(6), 840. https://doi.org/10.3390/w14060840

Boogaard, F., Bruins, G., Wentink, R., & Stichting RIONED. (2006). *Wadi's: aanbevelingen voor ontwerp, aanleg en beheer*. Stichting RIONED, Ede.

Bot, A.P. (2011). *Grondwaterzakboekje.* Bot Raadgevend Ingenieur.

Bouwens, C., ten Veldhuis, M.-C., Schleiss, M., Tian, X., & Schepers, J. (2018). Towards identification of critical rainfall thresholds for urban pluvial flooding prediction based on crowdsourced flood observations. *Hydrology and Earth System Sciences Discussions*. https://doi.org/10.5194/hess-2017-751

Bouwer, H. (1978). *Groundwater hydrology.* McGraw-Hill, New York.

Brooks, R. H., and Corey, A. T. (1964). Hydraulic properties of porous media *Hydro. Paper No. 3*, Colorado State Univ., Fort Collins, Colo.

Brown, G. O. (2002). Henry Darcy and the making of a law. *Water Resources Research*, *38*(7). https://doi.org/10.1029/2001WR000727

Davis, A. P. (2008). Field Performance of Bioretention: Hydrology Impacts. *Journal of Hydrologic Engineering*, *13*(2), 90–95. https://doi.org/10.1061/(ASCE)1084-0699(2008)13:2(90)

Ebrahimian, A., Sample-Lord, K., Wadzuk, B., & Traver, R. (2020). Temporal and spatial variation of infiltration in urban green infrastructure. *Hydrological Processes*, *34*(4), 1016–1034. https://doi.org/10.1002/hyp.13641

Elçi, A., & Molz, F. J. (2009). Identification of Lateral Macropore Flow in a Forested Riparian Wetland through Numerical Simulation of a Subsurface Tracer Experiment. *Water, Air, and Soil Pollution*, *197*(1), 149–164. https://doi.org/10.1007/s11270-008-9798-5

Emerson, C. H., & Traver, R. G. (2008). Multiyear and Seasonal Variation of Infiltration from Storm-Water Best Management Practices. *Journal of Irrigation and Drainage Engineering*, *134*(5), 598–605. https://doi.org/10.1061/(ASCE)0733-9437(2008)134:5(598)

Farthing, M. W., & Ogden, F. L. (2017). Numerical Solution of Richards' Equation: A Review of Advances and Challenges. *Soil Science Society of America Journal*, *81*(6), 1257–1269. https://doi.org/10.2136/sssaj2017.02.0058

Flury, M., Flühler, H., Jury, W. A., & Leuenberger, J. (1994). Susceptibility of soils to preferential flow of water: A field study. *Water Resources Research*, *30*(7), 1945–1954. https://doi.org/10.1029/94wr00871

Germer, K., & Braun, J. (2015). Determination of Anisotropic Saturated Hydraulic Conductivity of a Macroporous Slope Soil. *Soil Science Society of America Journal*, *79*(6), 1528–1536. https://doi.org/10.2136/sssaj2015.02.0071

Ghasemizade, M., Moeck, C., & Schirmer, M. (2015). The effect of model complexity in simulating unsaturated zone flow processes on recharge estimation at varying time scales. *Journal of Hydrology*, *529*, 1173–1184. https://doi.org/10.1016/j.jhydrol.2015.09.027

Gijsman, A. J., Thornton, P. K., & Hoogenboom, G. (2007). Using the WISE database to parameterize soil inputs for crop simulation models. *Computers and Electronics in Agriculture*, *56*(2), 85–100. https://doi.org/10.1016/j.compag.2007.01.001

Goede, J. (2022). *Wadi-Zenostraat Rotterdam BMP.* https://climatescan.nl/projects/3107/detail

Haghighatafshar, S., Yamanee-Nolin, M., & Larson, M. (2019). A physically based model for mesoscale SuDS – an alternative to large-scale urban drainage simulations. *Journal of Environmental Management*, *240*, 527–536. https://doi.org/10.1016/j.jenvman.2019.03.037

Harbaugh, A. W. (2005). MODFLOW-2005 : the U.S. Geological Survey modular ground-water model--the ground-water flow process. https://doi.org/10.3133/tm6a16

Hendrickx, J., & Flury, M. (2001). Uniform and Preferential Flow Mechanisms in the Vadose Zone. In *Conceptual Models of Flow and Transport in the Fractured Vadose Zone*. 149–187. National Academies Press. https://doi.org/10.17226/10102

Hillel, D. (1998). *Environmental soil physics*. Academic, San Diego.

Hunt, R. J., Prudic, D. E., Walker, J. F., & Anderson, M. P. (2008). Importance of Unsaturated Zone Flow for Simulating Recharge in a Humid Climate. *Ground Water, 46*(4), 551–560. https://doi.org/10.1111/j.1745-6584.2007.00427.x

Hurford, A. P., Priest, S. J., Parker, D. J., & Lumbroso, D. M. (2011). The effectiveness of extreme rainfall alerts in predicting surface water flooding in England and Wales. *International Journal of Climatology*, *32*(11), 1768–1774. https://doi.org/10.1002/joc.2391

IPCC. (2023). Summary for Policymakers. In: *Climate Change 2023: Synthesis Report. Contribution of Working Groups I, II and III to the Sixth Assessment Report of the Intergovernmental Panel on Climate Change* [Core Writing Team, H. Lee and J. Romero (eds.)]. IPCC, Geneva, Switzerland, 1-34, https://doi.org/10.59327/IPCC/AR6-9789291691647.001

Jain, S. K., & Sudheer, K. P. (2008). Fitting of Hydrologic Models: A Close Look at the Nash–Sutcliffe Index. *Journal of Hydrologic Engineering*, *13*(10), 981–986. https://doi.org/10.1061/(ASCE)1084-0699(2008)13:10(981)

Kaykhosravi, S., Khan, U. T., & Jadidi, A. (2018). A comprehensive review of low impact development models for research, conceptual, preliminary and detailed design applications. *Water*, *10*(11), 1541. https://doi.org/10.3390/w10111541

KNMI. (2015). *KNMI'14 climate scenarios for the Netherlands; A guide for professionals in climate adaptation*, KNMI, De Bilt, The Netherlands, 34 pp

KNMI. (2023). *KNMI'23-klimaatscenario's voor Nederland*, KNMI, De Bilt, KNMI-Publicatie 23-03.

KNMI. (2024). *KNMI - Winter 2023-2024 (december, januari, februari)*. https://www.knmi.nl/nederland-nu/klimatologie/maand-en-seizoensoverzichten/2024/winter

Kondratenko, J., Boogaard, F. C., Rubulis, J., & Maļinovskis, K. (2024). Spatial and Temporal Variability in Bioswale Infiltration Rate Observed during Full-Scale Infiltration Tests: Case Study in Riga Latvia. *Water*, *16*(16), 2219. https://doi.org/10.3390/w16162219

Koning, J., & Boogaard, F. C. (2023). Mapping, Assessing, and Evaluating the Effectiveness of Urban Nature-Based Solutions to Climate Change Effects in the Netherlands. In W. Leal Filho, G. J. Nagy, & D. Y. Ayal (Eds.), *Handbook of Nature-Based Solutions to Mitigation and Adaptation to Climate Change* (pp. 1–32). Springer International Publishing. https://doi.org/10.1007/978-3-030-98067-2_104-1

Kumar, P., Debele, S. E., Sahani, J., Rawat, N., Marti-Cardona, B., Alfieri, S. M., Basu, B., Basu, A. S., Bowyer, P., Charizopoulos, N., Gallotti, G., Jaakko, J., Leo, L. S., Loupis, M., Menenti, M., Mickovski, S. B., Mun, S.-J., Gonzalez-Ollauri, A., Pfeiffer, J., … Zieher, T. (2021). Nature-based solutions efficiency evaluation against natural hazards: Modelling methods, advantages and limitations. *Science of The Total Environment*, *784*, 147058. https://doi.org/10.1016/j.scitotenv.2021.147058

Lenhart, T., Eckhardt, K., Fohrer, N., & Frede, H.-G. (2002). Comparison of two different approaches of sensitivity analysis. *Physics and Chemistry of the Earth, Parts A/B/C*, *27*(9), 645–654. https://doi.org/10.1016/S1474-7065(02)00049-9

Leterme, B., Gedeon, M., Laloy, E., & Rogiers, B. (2015). Unsaturated flow modeling with HYDRUS and UZF: calibration and intercomparison. *MODFLOW and More 2015, Goden, CO, 5.*

Lewis, J., Hatt, B. E., Deletic, A., & Fletcher, T. D. (2008). The impact of vegetation on the hydraulic conductivity of stormwater biofiltration systems. In A. Saul, & et al (Eds.), *Proceedings of the 11th Int. Conf. on Urban Drainage (11ICUD)* (pp. 1 - 10). IWA Publishing.

Liao, K., Xu, S., Wu, J., & Zhu, Q. (2014). Uncertainty analysis for large-scale prediction of the van Genuchten soil-water retention parameters with pedotransfer functions. *Soil Research*, *52*(5), 431. https://doi.org/10.1071/SR13230

Metz, M. (2022). *Assessing the hydrologic performance of the Aquaflow in Rotterdam: A monitoring case study of the Agniesebuurt area of Rotterdam* [Master thesis, Delft University of Technology]. https://repository.tudelft.nl/islandora/object/uuid%3A453d0276-8ba4-4f09-971f-9a80d10020fd

Mirus, B. B., & Nimmo, J. R. (2013). Balancing practicality and hydrologic realism: A parsimonious approach for simulating rapid groundwater recharge via unsaturated-zone preferential flow. *Water Resources Research*, *49*(3), 1458–1465. https://doi.org/10.1002/wrcr.20141

Mobron, N. (2019). *Hydraulic functioning of bioswales under polder conditions: A field-survey in Rotterdam* [Master thesis, Delft University of Technology]. https://repository.tudelft.nl/islandora/object/uuid%3A0568be5a-b79f-4869-be45-5b95a695cd16

Mobron, N. (2024). *Rotterdamse wadi bouwsteen*.

Nash, J. E., & Sutcliffe, J. V. (1970). River flow forecasting through conceptual models part I — A discussion of principles. *Journal of Hydrology*, *10*(3), 282–290. https://doi.org/10.1016/0022-1694(70)90255-6

Nimmo, J. R. (2021). The processes of preferential flow in the unsaturated zone. *Soil Science Society of America Journal, 85*(1), 1–27. https://doi.org/10.1002/saj2.20143

Niswonger, R., Prudic, D., & Regan, R. (2006). Documentation of the Unsaturated-Zone Flow (UZF1) Package for Modeling Unsaturated Flow between the Land Surface and the Water Table with MODFLOW-2005. *US Geological Survey Techniques and Methods 6-A19*. Reston, Virgina: USGS.

Penman, H. L. (1948). Natural evaporation from open water, bare soil and grass. *Proceedings of the Royal Society of London a Mathematical and Physical Sciences*, *193*(1032), 120–145. https://doi.org/10.1098/rspa.1948.0037

Richards, L. A. (1931). CAPILLARY CONDUCTION OF LIQUIDS THROUGH POROUS MEDIUMS. *Physics*, *1*(5), 318–333. https://doi.org/10.1063/1.1745010

Ritter, A., & Muñoz-Carpena, R. (2013). Performance evaluation of hydrological models: Statistical significance for reducing subjectivity in goodness-of-fit assessments. *Journal of Hydrology*, *480*, 33–45. https://doi.org/10.1016/j.jhydrol.2012.12.004

Rujner, H., Leonhardt, G., Perttu, A.-M., Marsalek, J., & Viklander, M. (2016). *Advancing green infrastructure design: Field evaluation of grassed urban drainage swales*. Novatech 2016 - 9ème Conférence internationale sur les techniques et stratégies pour la gestion durable de l'Eau dans la Ville / 9th International Conference on planning and technologies for sustainable management of Water in the City, Jun 2016, Lyon, France. https://hal.science/hal-03322090

Schaap, M. G., Leij, F. J., & van Genuchten, M. Th. (2001). rosetta: A computer program for estimating soil hydraulic parameters with hierarchical pedotransfer functions. *Journal of Hydrology*, *251*(3), 163–176. https://doi.org/10.1016/S0022-1694(01)00466-8

Schaap, M. G., & van Genuchten, M. Th. (2006). A Modified Mualem–van Genuchten Formulation for Improved Description of the Hydraulic Conductivity Near Saturation. *Vadose Zone Journal*, *5*(1), 27–34. https://doi.org/10.2136/vzj2005.0005

Sela, G. (2024). *Using soil moisture sensors for irrigation management | Cropaia*. Cropaia. https://cropaia.com/blog/irrigation-management-soil-moisture-sensors/

Smedema, L.K. and Rycroft, D.W. (1983). *Land Drainage-Planning and Design of Agricultural Drainage Systems.* Cornell University Press, Ithaca, New York.

Spekkers, M. H., Clemens, F. H. L. R., & Veldhuis, J. a. E. T. (2015). On the occurrence of rainstorm damage based on home insurance and weather data. *Natural Hazards and Earth System Sciences*, *15*(2), 261–272. https://doi.org/10.5194/nhess-15-261-2015

Stumpp, C., & Kammerer, G. (2022). The Vadose Zone—A Semi-Aquatic Ecosystem. In T. Mehner & K. Tockner (Eds.), *Encyclopedia of Inland Waters (Second Edition)* (pp. 331–338). Elsevier. https://doi.org/10.1016/B978-0-12-819166-8.00179-1

Vaes, G., Berlamont, J. (1996). Composietbuien als neerslaginvoer voor rioleringsberekeningen. *Water*, *88*.

Van Genuchten, M. T. (1980). A Closed-form Equation for Predicting the Hydraulic Conductivity of Unsaturated Soils. *Soil Science Society of America Journal*, *44*(5), 892–898. https://doi.org/10.2136/sssaj1980.03615995004400050002x

Vereecken, H., Weihermüller, L., Assouline, S., Šimůnek, J., Verhoef, A., Herbst, M., Archer, N., Mohanty, B., Montzka, C., Vanderborght, J., Balsamo, G., Bechtold, M., Boone, A., Chadburn, S., Cuntz, M., Decharme, B., Ducharne, A., Ek, M., Garrigues, S., … Xue, Y. (2019). Infiltration from the Pedon to Global Grid Scales: An Overview and Outlook for Land Surface Modeling. *Vadose Zone Journal, 18*(1), 1–53. https://doi.org/10.2136/vzj2018.10.0191

Waterschap Hollandse Delta. (2020). *Waterbeheer programma 2022-2027*.

Woods Ballard, B., Wilson, S., Udale-Clarke, H., Illman, S., Scott, T., Ashley, R., Kellagher, R. (2015). *The SUDS manual.* CIRIA.

Zell, C., Kellner, E., & Hubbart, J. A. (2015). Forested and agricultural land use impacts on subsurface floodplain storage capacity using coupled vadose zone-saturated zone modeling. *Environmental Earth Sciences, 74*(10), 7215–7228. https://doi.org/10.1007/s12665-015-4700-4

Zhang, K., & Chui, T. F. M. (2020). Assessing the impact of spatial allocation of bioretention cells on shallow groundwater – An integrated surface-subsurface catchment-scale analysis with SWMM-MODFLOW. *Journal of Hydrology*, *586*, 124910. https://doi.org/10.1016/j.jhydrol.2020.124910

Appendix A. Overview of model parameters

Table A.1: Parameters per soil layer

Parameter	Description
K_h	Saturated horizontal hydraulic conductivity (m/d)
$K_{v,}$	Saturated vertical hydraulic conductivity (m/d)
ε	Brooks-Corey exponent (epsilon) (-)
S_y	Specific yield (-)
S_s	Specific storage (m^{-1})
Θ_r	Residual moisture content (-)
Θs	Saturated moisture content (-)
Surfdepth	Surface depression depth (m)
GW	Initial groundwater level (m NAP)

Table A.2: Drain parameters

Parameter	Description
Width	Width of the drain (m)
Inf_{factor}	Drainage vs infiltration factor (-)
Bottom	Bottom level of drain (m NAP)
Stage	Drainage level (m NAP)
C_{drain}	Drain entry-resistance (d)

Table A.2: Bioswale parameters

Parameter	Description
dz	Discretization of water ponding in bioswale (m)
Z_{max}	Overflow level (m NAP)
Inf_{rate}	Infiltration rate of bioswale (m/d)
C_{bottom}	Bottom conductance of bioswale (d)

Appendix B. Monte Carlo simulations

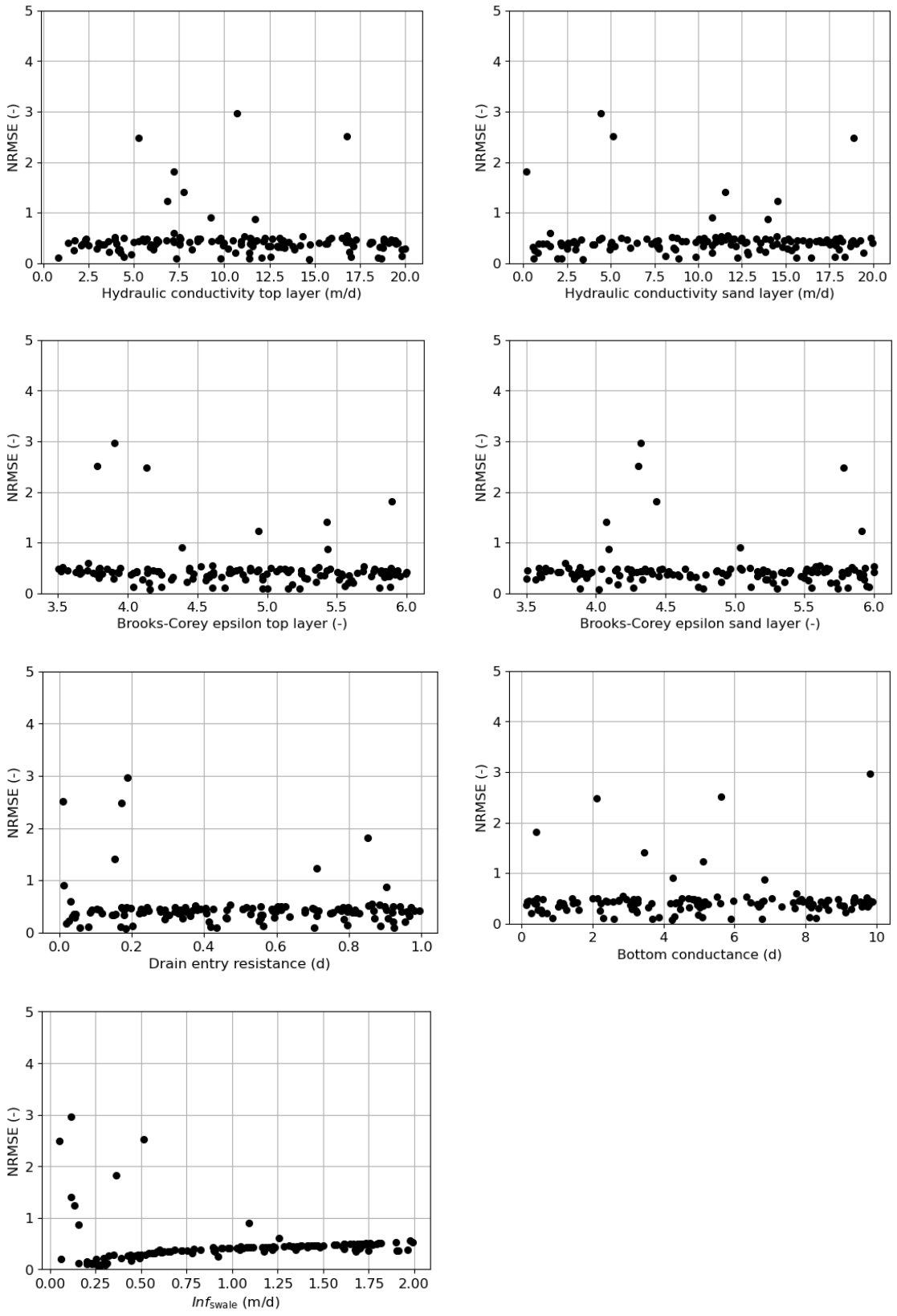

Figure B.0.1 NRMSE from Monte-Carlo simulation compared to the calibration parameters

Appendix C. Residual moisture content analysis

The residual moisture content in the Brooks-Corey equation, used in the Unsaturated Zone Flow (UZF) package of MODFLOW, can be interpreted as the water content remaining in the soil after gravitational drainage, which resembles field-capacity conditions. This analysis identifies the residual moisture content values that can be used as field capacity values based on soil texture measurements from the case study bioswale (Mobron, 2019) analysed in this study.

To relate moisture content to specific matric potentials for field-capacity conditions, water retention curves are computed. Using the Rosetta Lite DLL (Dynamically Linked Library) in Hydrus 1D, the Van Genuchten (1980) water retention parameters are predicted through pedotransfer functions (PTFs). Mobron (2019) collected soil samples from various layers of the bioswale, and the proportions of sand, silt, and clay were determined in the laboratory. These percentages are input into Rosetta to generate water retention curves. However, there is some uncertainty in predicting these parameters using neural networks (Liao et al., 2014; Schaap et al., 2001). Additionally, minor variations in the measured soil texture, possibly due to soil heterogeneity, could also contribute to the uncertainty. To account for this, uncertainty bounds are created along the water retention curves for different soil types. The soil texture measurements are plotted on the soil texture triangle (see Figure C.1, topsoil measurements), where a red circle corresponds to a 5% variation in soil texture composition to account for uncertainty.

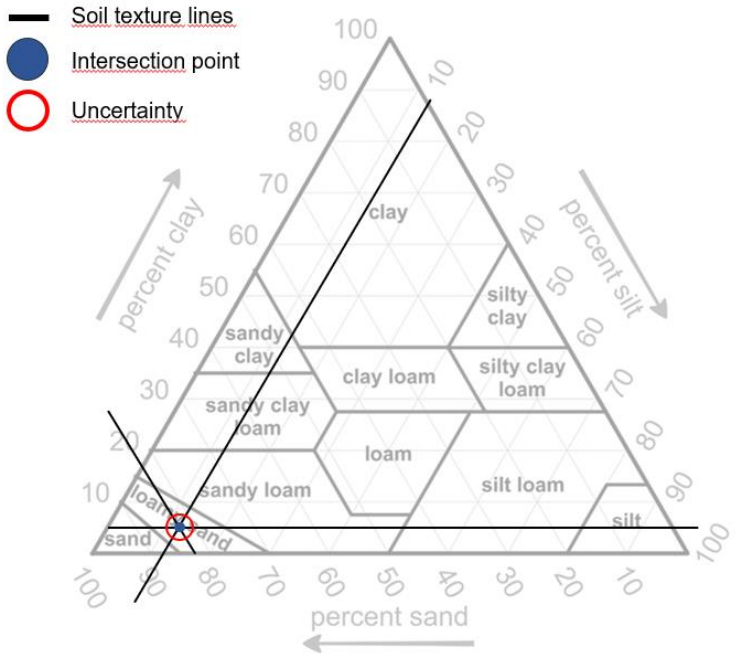

Figure C.1: Soil texture triangle with location of topsoil characteristics of the case study bioswale

Based on the outer points of the red circle in Figure C.1, different water retention curves are computed based on the predicted Van Genuchten parameters with Rosetta Lite DLL. In these curves, the Van Genuchten parameters θ_r and θ_s are kept constant as they have minimal influence on the curve's shape and slope, while only the scale and shape parameters, α and n, are varied. The order of magnitude for α and n values is consistent with the standard deviation found by Liao et al. (2014) for predicting Van Genuchten parameters using pedotransfer functions. The inner and

outer curves are selected, and for the top soil layer, this resulted in the water retention curves shown in Figure C.2. When a pF value between 1.9 and 2.1 is used for field capacity, the resulting range in moisture content for the topsoil layer is between 0.09 and 0.21 (see Figure C.3).

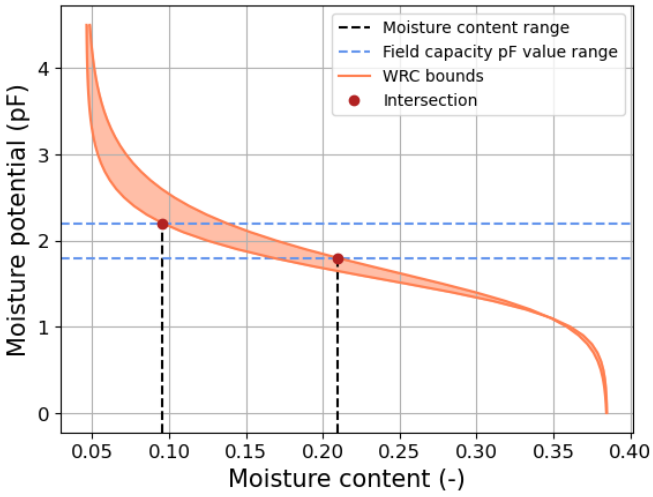

Figure C.2: Ranges of water retention curves top layer

The same analysis is conducted for the sand layer in the case study bioswale, resulting in a moisture content range between 0.05 and 0.14 (see Figure C.3).

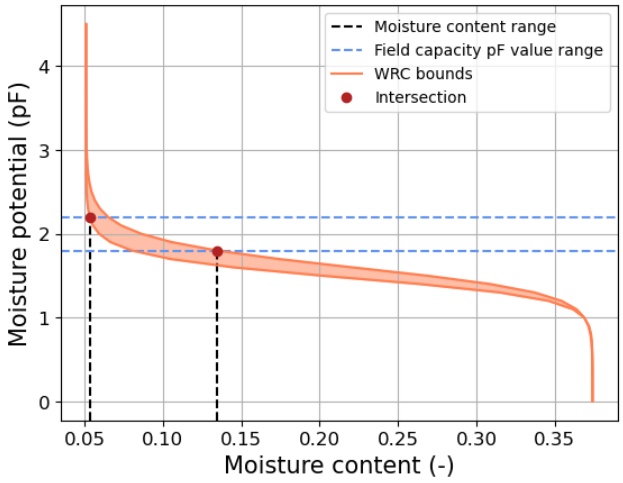

Figure C.3: Ranges of water retention curves sand layer

These moisture content ranges for the top and sand layer of the case study bioswale can be used as input for the residual moisture content in the bioswale groundwater model. This methodology can be applied to other bioswales if soil texture distribution is expected to vary. When the moisture content ranges from Figure C.2 and Figure C.3 are applied as residual moisture content (and initial) moisture content values for the T=2 years in 2014 design storm in summer (see Figure 3.5), the following outflow discharge curves are obtained (see Figure C.4). As shown in Figure C.4, the arrival time is shorter with higher residual moisture content, and the peak discharge increases accordingly.

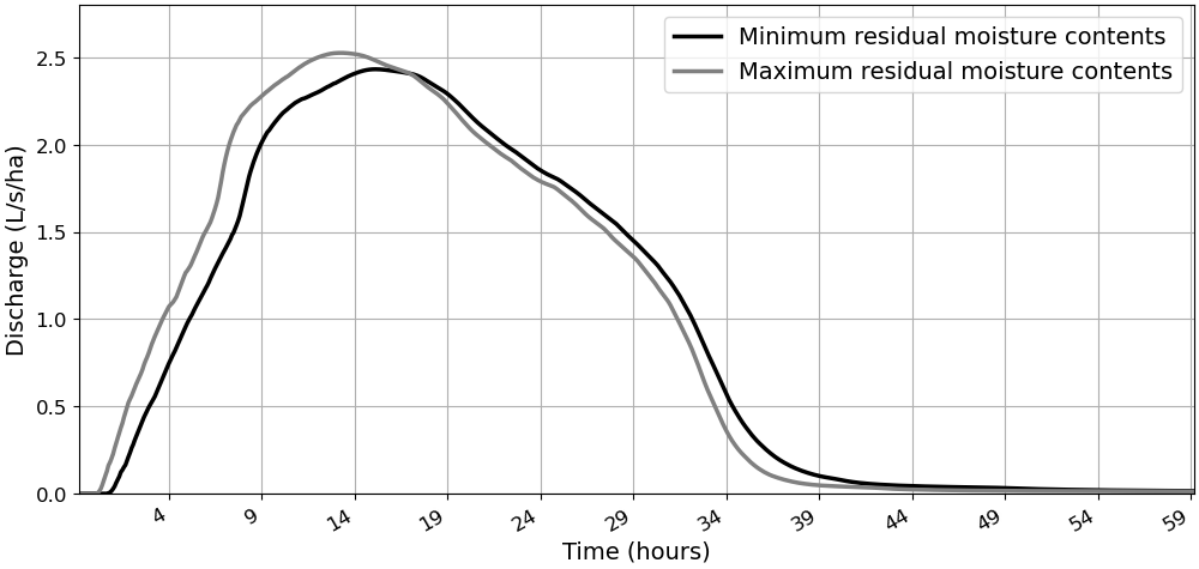

Figure C.4: Modelled outflow discharge for residual theta ranges

Appendix D. Rainfall measurements

Three different rainfall measurement sources are available in Rotterdam. The KNMI measures hourly rainfall at Zestienhoven (Rotterdam airport). A radar on the roof of the Delftse Poort building in Rotterdam records rainfall every 15 minutes at a height of 150 meters. Additionally, a rain gauge operated by the Municipality of Rotterdam at Grotekerkplein measures rainfall every 5 minutes. Figure D.1 below presents the hourly rainfall totals recorded by these sources between November 2023 and February 2024 and illustrates the variability in rainfall data across these sources. These differences can be attributed to errors in rainfall monitoring related to installation location and external factors such as wind speed and direction. As shown in Figure D.1 the rain gauge data is missing measurements for the beginning of November. The figure highlights variability between the different data sets. For instance, the rainfall station measurements often show higher peak values compared to the radar and KNMI measurements.

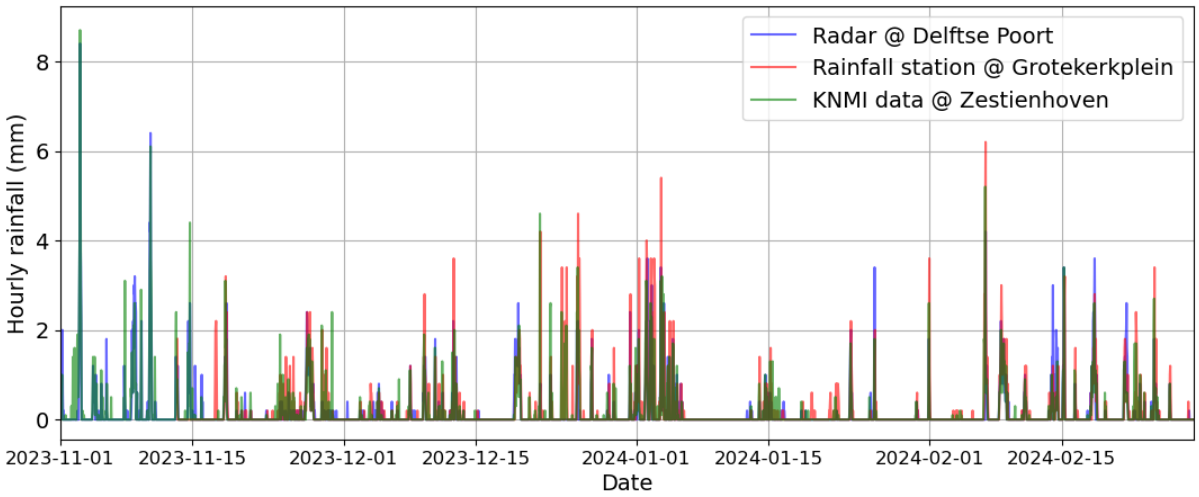

Figure D.1: Rainfall measurements in Rotterdam November 2023 - February 2024

Appendix E. Bioswale measurements March 2019 and April 2022

Students from Hanzehogeschool Groningen (Goede, 2022) measured the infiltration rate of the case-study bioswale in April 2022. The methodology was similar to that used in measurements conducted by Mobron (2019) in March/April 2019: full-scale test the same volume of storm 1 and 2 (30 m^3). The water levels measured in March 2019 and April 2022 are shown in Figure E.1 below.

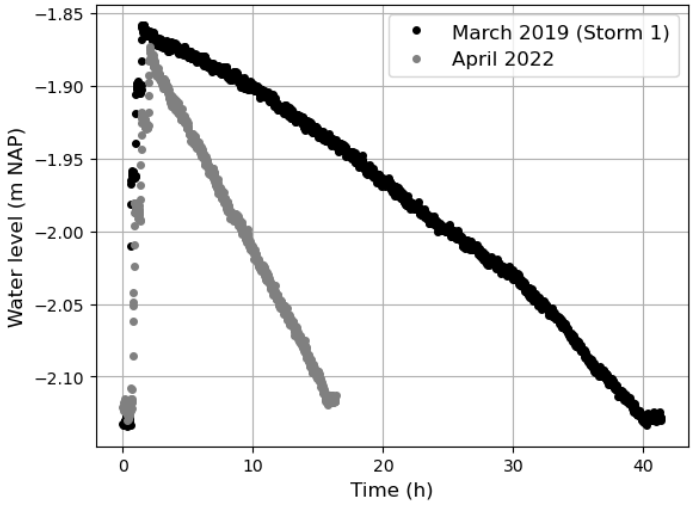

Figure E.1: Full-scale test measurements in case-study bioswale

As shown in Figure E.1, the infiltration of a similar volume of water was twice as fast in April 2022 compared to the measurements in March 2019. This difference can be attributed to several factors. First, the antecedent soil moisture conditions, though not measured, could have differed between the two periods, affecting the infiltration rate. Furthermore, the location of the diver used to measure the water level over time was not reported for the April 2022 measurements. A different placement of the measurement device could lead to different results. Additionally, a higher temperature in April 2022 may have contributed to the faster infiltration observed. Table E.1 presents the infiltration rates from the four full-scale tests conducted in 2019 by Mobron (2019) and the infiltration rate from the full-scale test in April 2022 (Goede, 2022), along with the air temperature recorded by divers prior to the full-scale tests.

Table E.1: Measured in filtration rate and air temperature of full-scale tests

Full-scale test	Date	Temperature	Infiltration rate (cm/h)
Storm 1	26-03-2019	7.8	0.697
Storm 2	21-03-2019	7.9	0.753
Storm 3	09-04-2019	10.2	0.678
Storm 4	28-03-2019	12.3	0.957
Test 2022	20-04-2022	18.8	1.802

The temperature and infiltration rate in April 2022 were noticeably higher compared to the full-scale tests conducted in 2019. This higher temperature can increase soil hydraulic conductivity, resulting in faster infiltration. Additionally, vegetation roots may have been more developed in April 2022 compared to March 2019, due to seasonal differences. This potential variation in vegetation could have led to the formation of larger macropores, contributing to the faster infiltration observed in April 2022. While no analysis of vegetation or macropores was conducted in either study, this

remains an assumption. However, photos taken during the measurements (see Figures E.2 and E.3) suggest denser vegetation in March 2019, which may have contributed to the slower infiltration. Furthermore, the higher temperatures (from KNMI observations) observed in the days prior to the April 2022 measurements may have promoted greater vegetation growth and the formation of larger macropores, compared to the March 2019 measurements.

Figure E.2: Photo taken during measurements in March 2019

Figure E.3: Photo taken during measurements in April 2022

In the absence of additional measurements, the March 2019 data were used as the winter infiltration rate, and the April 2022 data as the summer infiltration rate in the bioswale performance assessment (see section 5.3.1).

Appendix F. Groundwater level fluctuations

Figure F.1 shows the locations of piezometers that are continuously measuring groundwater levels in the Zenobuurt in Rotterdam. The phreatic piezometers '132561-99' and '132561-5' are the closesed located with the case study bioswale (located between Epicurusstraat and Plotinusstraat).

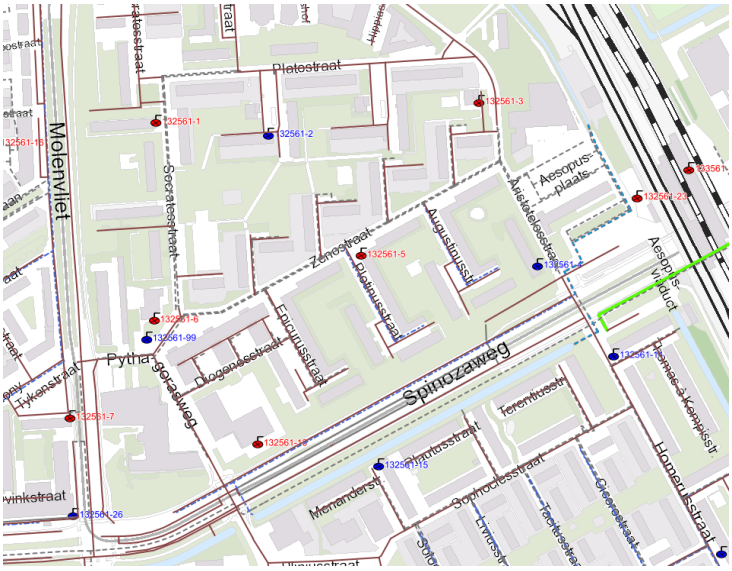

Figure F.1: Piezometer locations in the Zenobuurt, Rotterdam

The observed groundwater levels in time for these two piezometers is shown in the scatterplot in Figure F.2 below.

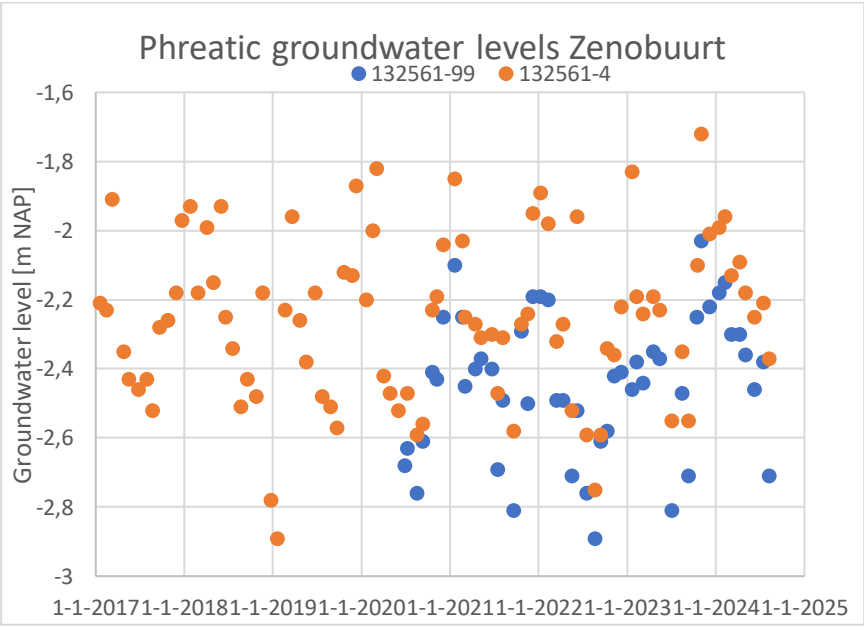

Figure F.2: Observed phreatic groundwater levels by two piezometers close to the case-study bioswale

Appendix G Weather scenario parameters and connected paved surface

From the methodology described in section 3.4.1 values for hydraulic conductivity, infiltration rate and groundwater levels have been determined. The calibrated values were used for winter conditions. From the model parameter sensitivity results it became clear that a two times as fast infiltration rate measured in summer conditions (see Appendix E) for the case-study bioswale can be attributed to an increase of Inf_{swale} parameter with 75%. Table G.1 shows the parameter values used to account for summer and winter conditions.

Table G.1: Model parameter values in summer and winter conditions

	Winter	Summer
Saturated hydraulic conductivity top layer (m/d)	15	22.5
Saturated hydraulic conductivity sand layer (m/d)	3.4	5.1
I_{swale} (m/d)	0.28	0.5

To evaluate the effect of initial groundwater levels in summer and winter conditions, initial groundwater levels of -2.7, -2.4 and -2.0 m NAP were evaluated, where -2.4 m NAP is the set drainage level in the area of the case-study bioswale. The other model parameters were kept constant between summer and winter scenarios, the calibrated parameter values in Table 5.1 and the parameter values in Table 4.1 were used.

The calculated runoff areas, including runoff from the gardens and additional connected paved surfaces, are shown in Figure G.2 below. In total, the runoff area covers 2006 m², with 617 m² being connected paved surface with a runoff coefficient (C) of 0.8, and 1389 m² from the gardens, with a runoff coefficient (C) of 0.3. The case-study bioswale itself occupies an area of 350 m².

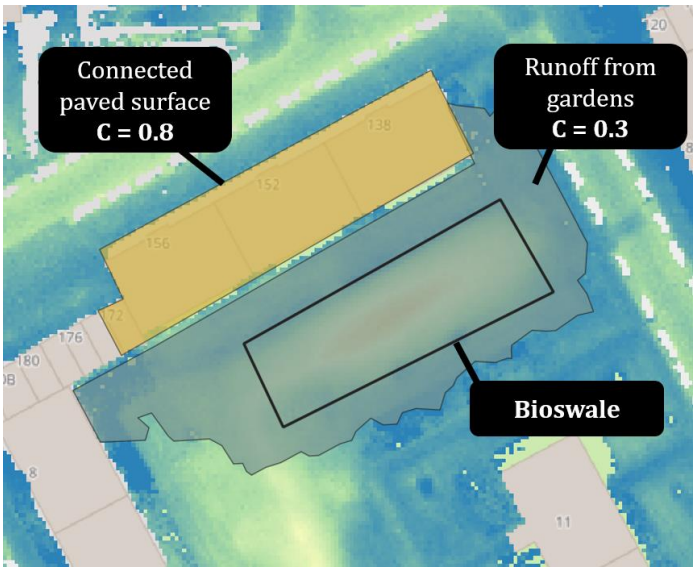

Figure G.2: Top view of case study-bioswale and calculated runoff areas